

PROJECT ADMINISTRATION DATA SHEET

ORIGINAL REVISION NO. _____

Project No. E-26-621 (continuation of E-26-659) DATE 2/5/82

Project Director: J. W. Poston School/Lab Nuclear Eng.

Sponsor: Department of Energy, Oak Ridge Operations

Type Agreement: Contract DE-AS05-79EV10248, Mod NO. A002

Award Period: From 2/1/82 To 1/31/83 (Performance) _____ (Reports)

Sponsor Amount: \$45,755 Contracted through: _____

Cost Sharing: None GTRI/GIT XXXX

Title: Experimental Verification of Internal Dosimetry Calculations

ADMINISTRATIVE DATA

OCA Contact William F. Brown x4820

1) Sponsor Technical Contact:

Dr. Wayne Lowder
US Dept. of Energy
Office of Health & Environmental Res.
Pollutant Characterization & Safety
Research Div.
Washington, DC 20545

2) Sponsor Admin/Contractual Matters:

Ms. Joyce Carringer
Procurement & Contracts Div.
Dept. of Energy
Oak Ridge Operations
Oak Ridge, TN 37830
(615) 576-7564

Defense Priority Rating: _____

Security Classification: _____

RESTRICTIONS

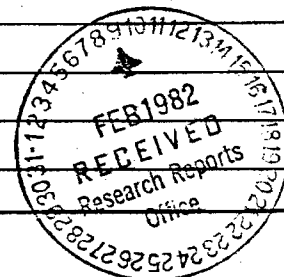
See Attached Gov't Supplemental Information Sheet for Additional Requirements.

Travel: Foreign travel must have prior approval - Contact OCA in each case. Domestic travel requires sponsor approval where total will exceed greater of \$500 or 125% of approved proposal budget category.

Equipment: Title vests with _____

COMMENTS:

Mod A002 adds \$45,744 through 1/31/83. Revised total contract value (including previous project number) is \$158,820.



COPIES TO:

Administrative Coordinator
Research Property Management
Accounting
Procurement/EES Supply Services
FORM OCA 4:781

Research Security Services
~~Reports Coordinator (OCA)~~
Legal Services (OCA)
Library

EES Public Relations (2)
Computer Input
Project File
Other _____

SPONSORED PROJECT TERMINATION/CLOSEOUT SHEET

Date 8/3/84

Project No. E-26-621 (Mod A002 - A006) School/Tab NE

Includes Subproject No.(s) _____

Project Director(s) Dr. J.W. Poston GTRI / GHT

Sponsor Department of Energy, Oak Ridge Operations

Title Experimental Verification of Internal Dosimetry Calculations

Effective Completion Date: 7/31/84 (Performance) 7/31/84 (Reports)

Grant/Contract Closeout Actions Remaining:

- None
- Final Invoice or Final Fiscal Report
- Closing Documents
- Final Report of Inventions
- Govt. Property Inventory & Related Certificate
- Classified Material Certificate
- Other _____

Continues Project No. E-26-659

Continued by Project No. E-25-618
Converted from Nuclear Engineering to Mechanical Engineering 7/1/84

COPIES TO:

- Project Director
- Research Administrative Network
- Research Property Management
- Accounting
- Procurement/EES Supply Services
- Research Security Services
- Reports Coordinator (OCA)
- Legal Services

- Library
- GTRI
- Research Communications (2)
- Project File
- Other I. Newton

SUMMARY OF PROGRESS

During the past year the research activities have been divided equally between experimental and calculational efforts. However, progress in the calculational area has been made quickly and some valuable data have been obtained. Significant strides in the experimental area have been slow in coming. These efforts are discussed individually below.

A. Absorbed Dose Distributions in Organs Constructed of PATE

The PATE dosimetry system has been used to provide volume averaged absorbed dose estimates for comparison to Monte Carlo calculations using the Snyder-Fisher phantom. These data were reported previously (3). In addition, the PATE system has the potential for use in providing absorbed dose distributions in the internal organs of the body. These dose distributions are of special interest in some of the large organs, such as liver, and also in organs located near the "source" organ(s) where there is a strong inverse square dependence in the radiation field intensity. It is clear that a better understanding of radionsensitive cells in certain organs will require a better estimate of the absorbed dose to certain critical cells or regions in these organs.

The PATE dosimetry system could be applied to this particular problem if a technique for sectioning the "organ dosimeters" could be developed. The technique must be relatively simple, easy to use, and must ensure that the TLD crystals incorporated in the tissue equivalent matrix are not thermally annealed during the sectioning (i.e., TLD crystals should not be heated to temperatures above about 100°C).

At this point little progress has been made toward solving this problem. The PATE mixture was, by design, a relatively hard material which could be subjected to rugged handling during the experiments. Attempts to design a device to section the mixture have provided only limited success.

Thermal cutting of the mixture was the first procedure tested. In all experiments the goal was to keep the bulk temperature of the PATE mixture below 100°C (the temperature of the TLD pre-read anneal).

Large organs could be cut easily with an electrically heated Nichrome wire. The wire, mounted on an insulated handle and heated to an appropriate temperature, could be passed easily through the organ. However, as the wire passed through the organ the "cut" made by the heated wire was quickly "healed" as the PATE system cooled rapidly to its solidification temperature (about 60°C). The net result was an intact organ, and sections of any reasonable size have not been obtained.

Modifications to this technique were tried to overcome the "healing" effect. For example, thin metal blades, electrically heated, were also tried in an effort to keep a larger area of the "cut" open at any one time. However, at this point, these attempts have not provided satisfactory results since the region continues to "heal" as the blade moves through the organ.

It is clear that a large heated blade for sectioning the organ is the solution to this problem. However, since the organs have various shapes

and the sensitive regions of the organs do not necessarily have simple shapes, this apparent solution does not truly provide the needed flexibility.

In other applications (see section B), the PATE system is sectioned into volumes of interest using a sharp knife. However, it is clear that this technique does not provide the kind of precision necessary for future work in this application nor in the extension to accurate extremity dosimetry.

Discussion with the faculty and staff of the School of Mechanical Engineering may provide additional possibilities for study.

Because of the lack of progress in this area, no experiments have been attempted inside the physical mock-up of the Snyder-Fisher phantom.

B. Use of PATE System for Extremity Dosimetry

The problem of obtaining accurate absorbed dose estimates for the extremities is a serious one and is still largely unresolved in routine personnel dosimetry (4,5,6). The particular difficulty with current techniques (finger and wrist dosimeters) is that the absorbed dose to the fingers, hands, and forearms must be estimated from point measurements supplied by these dosimeters. In addition, these dose estimates are complicated by the fact that the radiation fields, for which the estimates are required, usually have very steep dose gradients due to the inverse square relation. For these reasons, measurements obtained with finger or wrist dosimeters may not be indicative of the actual absorbed dose.

The PATE dosimetry system developed previously in this research presents an excellent opportunity to attack the extremity problem from a different angle. PATE, molded in the shapes of hands, can be exposed in a number of typical situations. Total dose and dose distributions in the hands can be obtained. These data can be compared to results obtained with finger and wrist dosimeters. The goal of this research is to provide a set of data which can be used to correlate the absorbed dose to the extremities to the dose measured by typical dosimeters.

During this year the primary effort has focused on molding techniques. However, some exposures, of an exploratory nature, have been made. Progress in this area is discussed below.

Preparing molds of the human hands is more complicated than techniques developed previously for the organs of the physical phantom. These organs had regular shapes and molds could be prepared easily by wrapping models of the organs with strips of plaster-of-paris tape(7). A mold of the human hand should, ideally, include individual regions for the thumb and four fingers. At the same time, it should be rugged due to the anticipated use.

Initial attempts to prepare a mold of the human hand used the plaster-of-paris strips mentioned above. Rubber gloves (size 8) were filled initially with paraffin to produce a solid structure around which the plaster strips could be wrapped. A layer of plaster strips was laid down on the glove completely enclosing the hand. To provide additional strength, extra layers of the plaster strips were added in the area of the fingers.

Although each finger was clearly defined inside the mold, the outer surface of the mold resembled a large mitten.

The mold was allowed to dry at room temperature on the laboratory bench. After the mold was dry and solid, a cast saw was used to remove it from the rubber glove-paraffin mold. Initial molds were quite fragile, primarily due to the need to have a realistic thumb, and other methods of molding were investigated.

One simple technique was to use a disposable surgeon's glove as the mold. A wire rim was fabricated to support the glove and to hold it open at the top. The PATE mixture was poured into the open glove and the glove was immersed immediately in a cold water bath. The bath promoted rapid solidification of the outer surface of the PATE and the entire PATE hand was completely hardened in about 20 minutes. At this point the surgeon's glove could be removed easily, revealing a smooth PATE hand.

However, several problems still remained. First, this simple procedure did not produce identical "hands" each time it was used. Second, the palm region of the hand was much too thick and was not truly representative of the human hand. Third, the fingers of the PATE hand nearly touched at the tips, another unrealistic situation.

To solve these problems and to have some control over the actual shape of the PATE hand, the two methods discussed above were combined. The surgeon's glove was retained as the primary mold but a plaster-of-

support was also prepared. The plaster support provided some structural rigidity in the region of the palm but did not cover any of the fingers. This combined technique provides a reproducible "hand", holds the fingers apart, and controls the thickness of the palm region. However, because of the use of plaster-of-paris, the water bath had to be abandoned. At this point the PATE mold is allowed to solidify overnight before use.

Two test exposures have been made to date using the PATE hands. The first exposure used a single hand oriented perpendicular to a beam of Co-60 gamma-rays. Distance from the source was 2.0 meters and the target exposure was 500 mR. The second exposure involved two hands oriented with the fingers of the hands pointing toward the source (i.e., the hands were oriented parallel to the beam). Again the distance from the source to the palms of the hands was 2.0 meters and the target exposure at the center of the palms was 500 mR. At this point, results are not available due to the large number of TLD samples that must be evaluated.

A cooperative program has been established with the Centers for Disease Control in Atlanta. The PATE hand dosimeter will be used to evaluate the absorbed doses to the fingers and hands of persons wearing radioactive gold jewelry.

The first reports on radioactive gold jewelry were published in the scientific literature in the late 1960's (8,9). The source of this radioactive gold is the use of spent radon seeds. Radon seeds, used for cancer therapy, are typically made of 24K gold. These seeds are tiny

hollow rods (wall thickness 0.3 mm), 0.75 mm in diameter and about 4.0 mm in length. Each seed has a mass of about 0.03 grams. During clinical use each seed may contain between 0.05 and 5 mCi of Rn-222. Although the seeds are no longer clinically useful, due to the decay of the short-lived radon, the gold seeds remain radioactive for a much longer period. One of the radon decay products is Pb-212, which has a half-life of 22.3 years.

It has been estimated that 100 to 200 gold seeds would be required to make a single gold wedding band (10). Dose rates to the basal layer of cells have been measured to be in the range 12 to 60 rads/day (8).

The cooperative research in this area involves using the PATE hands and placing radioactive gold jewelry on the hands for known periods of time. The PATE system can provide estimates of the absorbed dose to individual fingers and, if sectioning techniques can be worked out, dose distributions and estimates of the absorbed dose to sensitive cell layers. This research is being pursued with the cooperation of Ms. Christine Eheman (CDC) and Dr. G. D. Schmidt (CDRH). One ring has been obtained for use and at least one more ring will be shipped later. Because of molding problems no data has been obtained so far.

C. Development of a Realistic Head and Neck Region

The Snyder-Fisher phantom was designed more than 16 years ago and, in many

ways, reflects not only the computer capability at the time but also the areas of interest in nuclear medicine. For example, a number of agents are now used for brain-scanning, a procedure used more sparingly many years ago. The present phantom cannot be used to provide meaningful dose estimates for many of the newer procedures. A major effort has been devoted to the development of a more realistic head for incorporation in the computer code used for internal dose calculations. The realistic head for a 10-year old, proposed by Deus and Poston (11), was used as the model.

Assumptions

In the design of a more realistic head and neck region for the adult phantom, the following assumptions were made:

1. The total mass of the head and neck given by Snyder et al. (12) represents a realistic value and will be used as a target in the design.
2. The neck region represents about 1/8th of the total volume (and mass) of the region and the remaining 7/8ths is assigned to the head region.

These assumptions lead to the conclusion that the head and neck combined should have a total mass of 5083 g and a volume of 4655 cm³. Based on assumption 2, the design masses and volumes of the head and neck can be established. For the head, the design values are 4483 g and 4095 cm³. For the neck, the design values are 600 g and 560 cm³.

3. The dimensions of the various sections of the head may be obtained from ICRP 23(13) or through use of proportionalities with those of the ten-year old (11).
4. The heights of the head, trunk, and leg regions (i.e., the dimensions in the z-direction) in the the Snyder-Fisher phantom are correct and should not be modified in this design.

The phantom, as in previous discussions, is assumed to be erect and oriented in a Cartesian coordinate system. The origin of the coordinate system is taken as the center of the base of the trunk, the positive x-axis is directed to the phantom's left, the positive y-axis toward the posterior of the phantom, and the positive z-axis upwards through the head.

Description of Head and Neck Regions

Computer plots of the head and neck regions are shown in Appendix I and II for the y,z-plane and x,y-plane, respectively. Descriptions of the individual sections and components are given below:

Head region: The head region is a right elliptical cylinder topped by half an ellipsoid. The elliptical cylinder is cut by an inclined plane at the back of the head so the bottom base of the cylinder coincides with the top of the neck. For example, see the y,z plot with x=0 in Appendix I.

For $75.0 \leq z \leq 88$,

$$\left(\frac{x}{7.94}\right)^2 + \left(\frac{y}{10}\right)^2 \leq 1$$

If $y < 5$, then

$$\left(\frac{x}{7.94}\right)^2 + \left(\frac{y}{10}\right)^2 \leq 0.0336538462z - 1.96154 - \frac{(z-88)^2}{1405.003772}$$

For $88 \leq z \leq 94$,

$$\left(\frac{x}{7.94}\right)^2 + \left(\frac{y}{10}\right)^2 + \left(\frac{z-88}{6}\right)^2 \leq 1$$

The head has a volume of 4083.9 cm³ and a mass of 4507.3 g.

Neck region: The neck region is composed of tissue, thyroid, bone (part of the spine), and skin (2 mm thick). This region is represented by a circular cylinder given by:

$$70 \leq z \leq 75$$

$$x^2 + (y-1.49)^2 \leq 6.01$$

The volume of the neck is 567.37 cm^3 and it has a mass of 588.3 g.

Bone region: Regions containing bones include the cranium, face, mandible, lower and upper teeth, and the spine. Each of these is described below:

Cranium: The cranium is the volume between concentric ellipsoids cut by two inclined planes. The external shell is composed of two half ellipsoids having the same parameters along the x- and y-axes but different parameters along the z-axis. The internal shell is separated by a distance of 6.2 mm from the external shell. The volume of the cranium is 421.7 cm^3 and the mass is 626.7 g.

The external ellipsoids are given by:

$$88 \leq z \leq 93.8$$

$$\left(\frac{x}{7.74}\right)^2 + \left(\frac{y}{9.8}\right)^2 + \left(\frac{z-88}{5.8}\right)^2 \leq 1$$

$$81.1 \leq z \leq 88$$

$$\left(\frac{x}{7.74}\right)^2 + \left(\frac{y}{9.8}\right)^2 + \left(\frac{z-88}{6.9}\right)^2 \leq 1$$

and if $y \leq 0$, then

$$z \geq 81.1 - \left(\frac{6.9}{9.8}\right)y$$

The internal ellipsoids are defined by:

$$88 \leq z \leq 93.18$$

$$\left(\frac{x}{7.12}\right)^2 + \left(\frac{y}{9.18}\right)^2 + \left(\frac{z - 88}{5.18}\right)^2 \geq 1$$

$$81.1 \leq z \leq 88$$

$$\left(\frac{x}{7.12}\right)^2 + \left(\frac{y}{9.18}\right)^2 + \left(\frac{z - 88}{6.28}\right)^2 \geq 1$$

if $y \leq 0$, then

$$z \geq 81.72 - \left(\frac{6.9}{9.8}\right)y$$

Face: The face of the phantom is divided into two regions; the upper face (excluding the eyes and nares) and the upper teeth region.

The upper face region is described by a solid elliptical cylinder cut by an inclined plane, which defines the cranium, and vertical and horizontal planes, which separate the upper face region from the mandible and the upper teeth region, respectively. The equations defining this region are:

$$80 \leq z \leq 88$$

$$y - 4.05; \left(\frac{x}{6.93}\right)^2 + \left(\frac{y}{9.6}\right)^2 \leq 1$$

$$\text{If } \left(\frac{x}{7.74}\right)^2 + \left(\frac{y}{9.8}\right)^2 + \left(\frac{z - 88}{6.9}\right)^2 \leq 1,$$

$$\text{then } z \leq 81.1 - \left(\frac{6.9}{9.8}\right)y$$

The eyes and the nares are excluded from the region and are described by the following equations:

The eyes are assumed to be spheres

$$(x - 3.4)^2 + (y + 7.5)^2 + (z - 84.2)^2 \leq (1.22)^2$$

Both eyes have a volume of 15.2 cm^3 and a total mass of 15 g.

Nasal regions: The nasal regions are defined by two half-horizontal elliptical cylinders oriented perpendicular to the x-axis. The cylinders are cut by the surface which defines the face region and the vertical plane which separates the face region from the mandible. The equations are:

$$\left(\frac{|x| - 0.21}{0.80}\right)^2 + \left(\frac{z - 82}{1.7}\right)^2 \leq 1 \quad \text{with } |x| \geq 0.21,$$

$$- 9.6 \left[1 - \left(\frac{4}{6.93}\right)^2 \right]^{\frac{1}{2}} \leq y \leq - 4.05$$

The nasal regions have a volume of 24.3 cm^3 and a mass of 24 g.

If the eyes and the nasal regions are excluded, the upper face region has a volume of 241.9 cm^3 and a mass of 359.5 g.

Upper Teeth Region: This region is assumed to be the volume between two concentric elliptical cylinders cut by three planes: two horizontal planes which define the boundaries of the bone region of the face and the lower teeth and one vertical plane which defines the mandible. The defining equations for this region are given by:

$$\left(\frac{x}{4.60}\right)^2 + \left(\frac{y + 4.05}{5.20}\right)^2 \leq 1$$

$$\left(\frac{x}{3.44}\right)^2 + \left(\frac{y + 4.05}{4.70}\right)^2 \leq 1$$

$$y \leq - 4.05$$

$$78.72 \leq z \leq 80$$

The volume of the upper teeth region is 15.6 cm^3 with a mass of 23.2 g.

Mandible: The mandible is divided into two parts: the region of the lower teeth and the remainder of the region.

The lower teeth region is similar to that for the upper teeth. This region is described as the volume between two concentric cylinders cut by three planes: two horizontal and one vertical. The defining equations are:

$$\left(\frac{x}{4.60}\right)^2 + \left(\frac{y + 4.05}{5.20}\right)^2 \leq 1$$

$$\left(\frac{x}{3.44}\right)^2 + \left(\frac{y + 4.05}{4.70}\right)^2 \leq 1$$

$$y \leq -4.05$$

$$77.44 \leq z \leq 78.72$$

The lower teeth region has a volume of 15.6 cm^3 and a mass of 23.2 g.

The region excluding the lower teeth is assumed to be the volume between three elliptical cylinders cut by two vertical planes (defined by $y = 0$ and $y = -4.05$), two inclined planes, and one horizontal plane. The equations defining this region are:

$$\left(\frac{x}{6.40}\right)^2 + \left(\frac{y + 4.05}{5.55}\right)^2 \leq 1$$

$$\left(\frac{x}{3.40}\right)^2 + \left(\frac{y + 4.05}{3.86}\right)^2 \leq 1$$

for $y \leq -4.05$ and $0.0625 y + 75.80 \leq z \leq 77.44$, and

$$\left(\frac{x}{6.40}\right)^2 + \left(\frac{y + 4.05}{5.55}\right)^2 \leq 1$$

$$\left(\frac{x}{4.20}\right)^2 + \left(\frac{y}{7.80}\right)^2 \leq 1$$

for $-4.05 \leq y \leq 0$ and $0.0625 y + 75.80 \leq z \leq 81.1 - \left(\frac{6.9}{9.8}\right)y$.

The volume of this region (excluding the lower teeth) is 183.5 cm^3 corresponding to a mass of 272.7 g.

Spine: The spine is represented by an elliptical cylinder bounded by the external ellipsoid which defines the cranium. The equations are:

$$75 \leq z \leq 88 - 6.9 \left[1 - \left(\frac{x}{7.74} \right)^2 + \left(\frac{y}{9.8} \right)^2 \right]^{\frac{1}{2}}$$

$$\left(\frac{x}{2.17} \right)^2 + \left(\frac{y - 3.7}{1.67} \right)^2 \leq 1$$

The volume of the spine is 134 cm^3 and its mass is 199 g.

Organs: In addition to the eyes and the nasal regions, two organs are defined. These are the brain and the thyroid gland.

The brain is contained in the inner shell of the cranium. It is described following the model proposed by Eckerman et al. (14) and consists of two regions: one region made of white matter and a second region consisting of a mixture of gray and white matter. The white matter region is 13% by weight of the total brain, whereas the mixed region contains 49% by weight gray matter and 37.2% by weight of white matter. The brain is represented by two half-ellipsoids, the lower half-ellipsoid cut by an inclined plane (see cranium). The white matter is defined by a centered ellipsoid divided into two hemispheres by a plane. The remainder is assumed to be composed of white and gray matter.

white matter region:

$$\left(\frac{x}{4.42}\right)^2 + \left(\frac{y}{6.48}\right)^2 + \left(\frac{z - 88}{2.48}\right)^2 \leq 1$$

where $-1.35 \leq x \leq 1.35$. The volume of the white matter is 200.9 cm³ with a mass of 198.3 g.

gray and white matter region:

If $z \geq 88$,

$$\left(\frac{x}{7.12}\right)^2 + \left(\frac{y}{9.18}\right)^2 + \left(\frac{z - 88}{5.18}\right)^2 \leq 1$$

and for $z < 88$,

$$\left(\frac{x}{7.12}\right)^2 + \left(\frac{y}{9.18}\right)^2 + \left(\frac{z - 88}{6.28}\right)^2 \leq 1$$

For this region, the volume defining the white matter is excluded. The volume of the gray and white matter region is 1266.1 cm³ and the mass is 1249.5 g. The total volume of the brain is 1467 cm³ and the mass is 1447.7g.

Thyroid gland: The lobes of the thyroid are represented as the volumes between two concentric cylinders cut by a surface. The thyroid is defined by:

$$x^2 + (y + 0.8)^2 \leq (2.19)^2$$

$$x^2 + (y + 0.8)^2 \geq 1$$

$$y + 0.80 \leq 0$$

$$70 \leq z \leq 74.75$$

$$\left[(y + 0.80) - |x|\right]^2 - z (x^2 + (y + 0.80)^2) \tau^2$$

$$\text{with } \tau = \frac{2(\sqrt{2} - 2)}{4.75} (z - 70) + 1 \text{ for } 0 \leq z - 70 \leq 71.25$$

$$\text{and } \tau = \frac{2(2 - \sqrt{2})}{14.25} (z - 70) + \frac{2\sqrt{2} + 1}{3} \text{ for } 1.25 \leq z - 70 \leq 4.75$$

The volume of the thyroid gland is 19.9 cm³ and the mass is 19.6 g.

Table 1 summarizes the volumes and masses of the organs and regions in this new design. Table 2 gives a comparison of the old and new regions. As stated previously, computer plots of the regions are given in Appendices I and II.

At this point, this new design is being coded into the existing Monte Carlo code. After debugging the modified code, it is anticipated that computer calculations will be undertaken for a large number of radionuclides. At this time, it is not clear that the calculations will be completed by the end of the project year (i.e., July 31, 1984).

D. Development of a Model of the Circulating Blood

Currently, the MIRD Committee of The Society of Nuclear Medicine has a great need for a model to describe the circulatory system in an adult human (15). This need exists because of the large number of radionuclides used in nuclear medicine which have short half-lives and only irradiate the body as they are carried throughout the body in the circulatory system. In addition, no model is available at present which describes concentrations of radionuclides in regions, such as the "face", which are fed primarily from the blood pool.

During this period a significant effort has been directed toward the development of a simple model of the circulating blood.

Description of the Blood Model

Initial data, on which the model was based, were selected from the Report on Reference Man (13). A total blood volume of 5200 ml was selected as being appropriate for a 70 kg adult. Table 3 gives the distribution of the blood in the total body based on this blood volume. Table 4 shows a more extensive breakdown on the blood distribution in the adult. The total volume obtained from this table ranges between 5103 and 5437 ml and, therefore, the 5200 ml value selected for the model is in apparent agreement with these data.

The Report on Reference Man (13) also presented data on the total blood volume in most organs of the body. These data were used to select those organs which should be included explicitly in the model. In addition, these data provided important guidance on those organs or regions of the body which could be combined into a single region in the model. Organs included in the blood model were the brain, heart, kidneys, liver, lungs and the spleen. Special regions, created for use in the simplified model, included the extremities, face, intestinal, aorta and vena cava, and the "remainder". Table 5 gives the total blood volume assumed to be in each organ or region of the model.

The organs named specifically in Table 5 are described mathematically by equations which were already part of the existing computer code. All other regions were designed especially for use in the model of the circulating blood. A short description of each of these regions is given below.

Extremities: The extremities are right circular cylinders, 1 cm. in diameter, located on the inside of the existing arm and leg bones. For example, the arm region lies between the existing arm bone and the ribs. It runs parallel to the bone region. Each arm region had a length of 69 cm. while each leg region was 79.8 cm. in length. The arm regions were moved forward 2.5 cm. along the y-axis to eliminate overlapping with the ribs.

$$\text{Arm regions: } \left[x \pm (17.9 - 0.02029z) \right]^2 + (y + 2.5)^2 \leq 0.5$$

$$0 \leq z \leq 69.$$

The + and - correspond to the right and left arm regions, respectively.

$$\text{Leg regions: } x \pm (6 + 0.06892z)^2 + y^2 \leq 0.5$$

$$-79.8 \leq z \leq 0.$$

Face region: The face region was assumed to be a region on the lower two-thirds of the head (i.e., $z \leq 85.5$). This region was formed by a plane which cut vertically through the elliptical cylinder of the head at $y = -7$. Care was taken in the definition of the face region to assure that there was no overlap between this region and the brain, another source organ.

$$-5 \leq x \leq 5$$

$$-7 \leq y \leq 0$$

$$70 \leq z \leq 85.5$$

$$\frac{x^2}{7} + \frac{y^2}{10} \leq 1$$

$$\frac{x^2}{6} + \frac{y^2}{9} + \frac{(z - 86.5)^2}{6.5} > 1.$$

The last equation excludes the brain from the face region.

Intestinal Region: The intestinal region was assumed to be located in the lower trunk constrained between $z = 0$ and $z = 27$. For simplicity the region was assumed to be represented by an elliptical cylinder with essentially the same dimensions as the trunk. However, the skin was not included in this region. The major axis of the elliptical cylinder was assumed to be 19.8 cm. and the minor axis was 9.8 cm. The center of this region, a circular region with the same height and a radius of 2.5 cm., was removed to bring the volume in line with the design parameters. Care was also taken that the intestinal region did not overlap with the aorta and vena cava region.

$$\begin{aligned}
 -x^2 + y^2 &\leq 2.5 \\
 \left(\frac{x}{19.6}\right)^2 + \left(\frac{y}{9.8}\right)^2 &\leq 1 \\
 0 &\leq z \leq 27.
 \end{aligned}$$

Aorta and Vena Cava: This region was described by a right circular cylinder with a radius of 2.5 cm. located between $z = 8$ and $z = 44.8$. Care was taken to eliminate overlap with the liver and heart source organs.

$$\begin{aligned}
 x^2 + y^2 &\leq (2.5)^2 \\
 \frac{x}{35} + \frac{y}{45} - \frac{z}{43} &\geq -1 \\
 8 &\leq z \leq 44.7761
 \end{aligned}$$

The second equation excludes the liver from the region whereas the last inequality excludes the heart.

Remainder: The "remainder" was assumed to be the total body, minus all other organs and regions mentioned above. This region was included to account for the essentially uniform distribution of a large fraction of the total blood volume in the body. A special source subroutine was prepared which allowed the selection of starting coordinates for photon histories uniformly throughout the phantom except in the organs and regions included explicitly in the model of the circulating blood.

Calculations of Absorbed Fractions

Using the model described above, computer calculations were performed for the 12 monoenergetic photon energies ranging from 0.01 to 4.0 MeV. In each calculation 60,000 photon histories were traced. Tables 6-8 present the absorbed fractions of energy for monoenergetic photon sources distributed uniformly in the model of the circulating blood. Tables 9-11 present the specific absorbed fractions for the same 12 monoenergetic photon sources.

U.S. DEPARTMENT OF ENERGY
UNIVERSITY-TYPE CONTRACTOR AND GRANTEE RECOMMENDATIONS
FOR DISPOSITION OF SCIENTIFIC AND TECHNICAL DOCUMENT

See Instructions on Reverse Side

1. DOE Report No.	3. Title
2. Contract No. DE-AS05-79EV10248	Experimental Verification of Internal Dosimetry Calculations

4. Type of Document ("X" one)
 a. Scientific and technical report
 b. Conference paper:
Title of conference _____
Date of conference _____
Exact location of conference _____
Sponsoring organization _____
 c. Other (Specify Thesis, Translations, etc.)

5. Recommended Announcement and Distribution ("X" one)
 a. DOE's normal announcement and distribution procedures may be followed.
 b. Make available only within DOE and to DOE contractors and other U.S. Government agencies and their contractors.

6. Reason for Recommended Restrictions

7. Patent Information
Does this information product disclose any new equipment, process or material? Yes No
Has an invention disclosure been submitted to DOE covering any aspect of this information product? If so, identify the DOE (or other) disclosure number and to whom the disclosure was submitted. Yes No
Are there any patent related objections to the release of this information product? If so, state these objections.

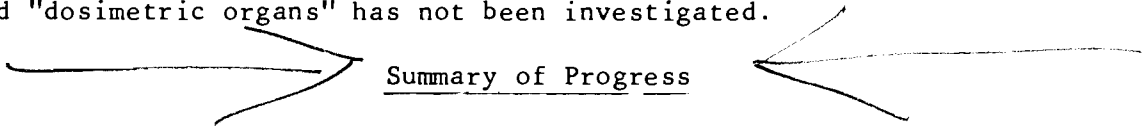
8. Submitted by Name and Position (Please print or type)
John W. Poston, Associate Professor
Organization
Georgia Institute of Technology
Signature _____ Date
May 2, 1983

FOR DOE USE ONLY

9. Patent Clearance ("x" one)
 a. DOE patent clearance has been granted by responsible DOE patent group.
 b. Report has been sent to responsible DOE patent group for clearance.
 c. Patent clearance not required.

terminated because of funding problems and not because of insurmountable technical problems.⁽¹⁶⁾

Before this method can be applied widely to the experimental determination of internal exposure conditions, additional research will be required. There has been some indication that the thermoluminescence properties of TLD materials may be changed after contact with organic liquids. For example, LiF has been suspended (or surrounded) in organic liquids with high hydrogen content to increase the TL response to fast neutrons.^(17,18) Puite⁽¹⁹⁾ performed a similar study with CaF_2 (Mn) suspended in organic liquids. Spurny and his colleagues⁽²⁰⁾ studied the effects on TL response of suspending LiF in water. The mechanism of the changes in response of TL materials in these liquids is not completely clear. The effects on TL response of suspending a TLD powder in an organic matrix (such as PAC) to mold "dosimetric organs" has not been investigated.



Summary of Progress

During the past year the dosimetry research program has continued in the School of Nuclear Engineering and Health Physics at the Georgia Institute of Technology. The major objective of this program has been to provide research results upon which a useful internal dosimetry system could be based. The important application of this dosimetry system will be the experimental verification of internal dosimetry calculations such as those published by the MIRD Committee^(1,2).

Specific research goals attained will be divided into several categories to discuss the progress in each area.

A. The Dosimetric System:

The detection system used in this research was the Pate dosimeter which derives its name from the mixture of paraffin and tetrachlorobenzene. The volumetric dosimeter contains 0.1% to 0.5% LiF TLD-100 powder, depending on the size of the organ. The chemical and elemental compositions of the mixture for a 0.5% TLD concentration are given in Table 1. For the lower concentrations, the ratio paraffin-tetrachlorobenzene remains constant. The dosimeter has a density of $0.96 \pm 0.01 \text{ g/cm}^3$ which is very close to the density of the MIRD tissue material (0.987 g/cm^3). Table 2 gives the different interaction coefficients for the Pate + 0.5% TLD-100 dosimeter, while Table 3 gives a comparison between these coefficients and those of the MIRD tissue. The MIRD tissue is that derived by Snyder and his colleagues and is therefore referred to in the table as "ORNL tissue"^(1,2,3).

Fabrication of Dosimetric Organs

Fabrication of a dosimetric organ starts by lining the walls of the two halves of the plaster bandage mold (see mold fabrication section) with aluminum foil to provide easy separation between the mold and the organ dosimeter. Preparation of the dosimeter itself requires special care to maintain the purity of the TLD powder and the composition of the mixture. The TLD powder has a 100-200 Tyler mesh crystal size. This crystal size is commercially available and it was chosen to achieve a more uniform distribution of the TLD powder in the organic mixture.

The procedure for preparing the Pate dosimetric organs is as follows: paraffin and tetrachlorobenzene are mixed in the specified proportions and melted in a beaker at a temperature of about 80°C . The

Table 1. General Characteristics of the Pate Organ Dosimeter

Composition:

TLD - 100	0.5%
$C_6H_2CL_4$	9.04
Paraffin	90.46%

Net Chemical Composition of Pate + 0.5% TLD 100

Element	Fraction
H	0.1334
LI	0.0013
C	0.8022
F	0.0037
CL	0.0594

Average Atomic Wt.: 11.9544

Number of Electrons Per Gram: 3.39638E+23

Effective Atomic Number: 7.39188

Average Molecular Wt.: 11.9544

TABLE 2. MASS ATTENUATION AND ABSORPTION COEFFICIENTS FOR PATE + 0.5% TLD-100

ENERGY (keV)	PHOTO. (cm ² /gm)	COHERENT	INCOHERENT	TOTAL ATTN.	ABSORPTION
10	49.9416E-01	18.6441E-02	16.7593E-02	53.4820E-01	49.9730E-01
15	14.4624E-01	10.7914E-02	18.5822E-02	17.3997E-01	14.5138E-01
20	59.0267E-02	70.7687E-03	19.3507E-02	85.4542E-02	59.7252E-02
30	16.4073E-02	37.3817E-03	19.6604E-02	39.8059E-02	17.4296E-02
40	65.6432E-03	23.1091E-03	19.3697E-02	28.2449E-02	78.5628E-03
50	32.1944E-03	15.6835E-03	18.8941E-02	23.6819E-02	47.4419E-03
60	17.9889E-03	11.3273E-03	18.3699E-02	21.3015E-02	35.2199E-03
80	71.9676E-04	66.8096E-04	17.3483E-02	18.7363E-02	27.5136E-03
100	35.5278E-04	43.8715E-04	16.4375E-02	17.2313E-02	26.2363E-03
150	10.0018E-04	20.0007E-04	14.6418E-02	14.9418E-02	27.5750E-03
200	41.3938E-05	11.2968E-04	13.3418E-02	13.4952E-02	29.2590E-03
300	12.3325E-05	49.7472E-05	11.5821E-02	11.6442E-02	31.3487E-03
400	53.7370E-06	27.5861E-05	10.4323E-02	10.4653E-02	32.3730E-03
500	28.7562E-06	17.4109E-05	96.1302E-03	96.3331E-03	32.9437E-03
600	17.4928E-06	11.9412E-05	89.9527E-03	90.0896E-03	33.0751E-03
800	82.0970E-07	55.8251E-05	81.1906E-03	81.2646E-03	33.2070E-03
1000	45.8422E-07	41.5034E-05	75.2344E-03	75.2805E-03	33.1003E-03

Table 3. COMPARISON OF PATE +0.5% TLD-100 WITH ORNL TISSUE

ENERGY (keV)	% PHOTO	% COHERENT	% INCOHERENT
10	0.7446	-29.5627	18.6732
15	7.9975	-28.8439	12.5420
20	12.5992	-28.2976	9.6425
30	18.1916	-27.5339	7.1709
40	21.5066	-27.0301	6.3313
50	23.7211	-26.6780	6.0907
60	25.3175	-26.4234	6.1086
80	27.4961	-26.0966	6.4367
100	28.9495	-25.9178	6.8660
150	31.2396	-25.7939	7.3032
200	32.7469	-25.8883	8.4042
300	34.9982	-26.3177	8.8396
400	36.8864	-26.8548	8.6548
500	38.6323	-27.4143	8.1265
600	40.3038	-27.9680	7.3994
800	43.5098	-29.0235	5.6391
1000	46.5911	-29.9978	3.7080

resulting mixture is screened through a 200 Tyler mesh sieve to remove unwanted impurities. The beaker is then placed in a 60°C water bath and allowed to cool until the temperature of the Pate compound equals that of the bath. At this stage, the Pate is in a semi-liquid, semi-solid state, and the TLD powder is added by sprinkling while mixing by hand. This manual mixing ensures a uniform distribution of the TLD crystals in the organ dosimeter (less than 3.4% variation in the concentration of the TLD powder in any part of the organ). The final step consists of overfilling the two halves of the plaster bandage mold and joining them together while the Pate dosimeter is still hot. After a short cooling period, the dosimetric organ is removed from the mold and is ready to be placed in the phantom for irradiation. Inspection of this complete organ shows good fusion of the two halves. There are no visible boundaries and the "fused" organ dosimeter exhibits similar physical characteristics to the organs molded in one pouring using a complete plaster bandage mold.⁽²¹⁾

The above organ fabrication procedure is used for all organs of unit density. However, in the case of the lungs, which have a density of 0.3 g/cm³, a different technique is used. After the screened Pate mixture has solidified, it is shredded in a food processor. TLD powder is added in small samples to the shredded Pate while stirring to obtain a uniform distribution of the TLD crystals. The final dosimetric mixture is poured in a lung container mold made of fiberglass. Fabrication of these containers is described in the section B dealing with the preparation of organ molds.

Once the irradiation of the dosimeter organs is accomplished, they are put through a procedure to recover the TLD powder. This procedure is described below.

TLD Powder Recovery Procedure

Several techniques were investigated for the recovery of the thermoluminescent powder for the organic mixture. The following procedure was chosen because it left the TLD crystals essentially free of impurities.

1. Put the Pate organ in a beaker and add carbon tetrachloride (CCl_4) in a 1:2 ratio.
2. Heat the mixture to a maximum temperature of 80°C .
3. Once the Pate has dissolved, pour the mixture (Pate + CCl_4) through the 200 Tyler mesh sieve.
4. Place the sieve in three separate dishes containing warm CCl_4 , for about 90 sec in each dish. This 3 stage purification should dissolve most of the Pate.
5. Place the sieve in a vacuum funnel and allow the crystals to air dry. It takes about 3 minutes for the TLD crystals to dry.
6. Hold the sieve above the last dish (see step 4 above), and wash the TLD crystals with CCl_4 from the wash bottle.
7. Repeat step 5; this time, the TLD crystals should be left to dry completely for about 6 minutes.
8. Put the TLD crystals into the 2 sieve screening system (3 inch diameter, the 100 mesh sieve on top of the 200 mesh sieve) and shake until the TLD powder is screened.

9. Pour the TLD powder on a piece of weighing paper and weigh; after weighing, place the TLD powder in a marked stainless steel dish for evaluation.

In the case of the lungs a different procedure for recovering the TLD powder without melting the organic mixture was attempted. This procedure consisted of screening the TLD powder and reusing the shredded Pate. The Pate mixture clogged the sieve and the above procedure had to be used to recover the TLD crystals.

A study was performed to determine the recovery rate of the TLD powder using the above procedures. Several samples were used and the data collected indicated that a recovery rate of at least 97% could be achieved. The loss of the TLD powder was mainly due to two factors: pulverization of the crystals to a size smaller than 200 Tyler mesh and adherence to the various pieces of equipment used in the experiment.

Reading Procedure:

The reading equipment consisted of a Harshaw TL detector, model 2000 A, and an automatic integrating picoammeter, model 2000 B.

The reading characteristics were:

High voltage: 700 volts

Preheat temperature: 100°C

Heating rate: 5.7°C/sec

Reading time: 30 sec

Maximum temperature 250°C

The electrically vibrated powder dispenser was used to measure each TLD sample to be read. This dispenser was calibrated using fresh TLD powder, and was found to have an accuracy of 3% with the mean weight of a dispensed sample being 13.875 mg. A better accuracy could probably

be achieved for situations involving a few samples, however this accuracy was considered acceptable considering the hundreds of samples which had to be evaluated in this research.

Annealing Procedure:

During each cycle, the TLD powder goes through two annealing procedures: a pre-annealing step before the TLD powder is mixed with the Pate compound serves the purpose of restoring the TLD crystals to their original characteristics, and a post-annealing step which is carried out after the TLD powder is recovered from the organic mixture. This latter step is required because of the instability of the low temperature peaks. In addition, this procedure ensured that all the TLD samples were treated the same way considering the temperature fluctuations that may occur during the recovery procedure. Post-annealing consisted of a period of 10 minutes at a temperature of 100°C.

Three experiments were carried out to determine the optimum pre-annealing procedures. In the first experiment, the TLD powder was annealed at 400°C for 1 hour and at 80°C for 24 hours with no cooling period in between. The second study consisted of an anneal for 1 hour at 400°C and 2 hours at 100°C with no cooling period, while in the third experiment, a cooling period of 15 minutes between the two heatings was used. The results obtained with the third annealing method were found to be reproducible. In addition, the TLD-100 showed a better sensitivity with the third annealing procedure.

TLD Distribution in Pate

Several methods of molding were investigated with an objective of achieving a uniform TLD crystal distribution in the Pate mixture. The first method consisted of melting the Pate in a beaker and adding the

TLD powder. The resulting mixture was poured into a right cylindrical mold "at once", and left to cool in a freezer. The inside of the cylindrical mold had a diameter of 5.3 cm and a height of 30 cm. After solidification, the Pate-TLD compound was removed from the mold and sliced into 13 sections. The thickness and mass of each slice were determined before attempting to recover the TLD-100 powder. The data obtained in this study are given in Table 4. Slice number 1 corresponds to the bottom of the cylinder, whereas slice number 13, is the upper portion of the cylinder. The extremely uneven distribution of the TLD-100 powder in the Pate mixture can be seen clearly in these data. The TLD concentration in the Pate can be characterized as following an exponential decrease from the bottom to the top of the cylinder.

The next attempt to obtain a uniform mixture of Pate and TLD crystals was made using ultrasound. The melted mixture was transferred to a beaker. The beaker was placed in a warm water bath which served as a conducting medium for the ultrasounds generated by a 300 W. transducer. The transducer was used to agitate the liquid Pate-TLD mixture for periods of more than one hour. In all cases, the TLD crystals remained on the bottom of the beaker where they had settled initially. For this reason, the experiment was terminated and no data were taken.

To overcome the above problems, a third method was devised. This method utilized a layering process which is described below:

- a. melt paraffin and $C_6H_2Cl_4$ at a temperature of about 80-100°C.
- b. pour this mixture through the 200 Tyler mesh screen.
- c. allow the mixture to solidify in a shallow stainless steel pan.

Table 4. TLD Distribution when Molding is Done in One Pouring

<u>Slice Number</u>	<u>Height (cm.)</u>	<u>Cumulative Height (cm.)</u>	<u>Weight (g)</u>	<u>TLD-100 Weight (g)</u>	<u>TLD Concentration (%)</u>
1	2.042	2.042	45.05492	7.51645	16.6829
2	1.431	3.473	31.57830	0.29480	0.9336
3	1.552	5.025	39.23465	0.13410	0.3917
4	1.137	6.162	25.08504	0.03795	0.1513
5	1.467	7.629	32.37079	0.03720	0.1149
6	1.082	8.711	23.87346	0.02165	0.0907
7	1.567	10.278	34.56629	0.02178	0.0360
8	1.532	11.810	33.79788	0.02650	0.0783
9	1.972	13.782	43.51380	0.02220	0.0510
10	1.562	15.644	34.46477	0.01388	0.0402
11	1.922	17.566	42.41088	0.01012	0.0239
12	1.455	19.021	32.09712	0.00005	0.0002
13	1.617	20.638	35.66424	0.01068	0.0299

Total weight of TLD recovered 8.14735 g

- d. when organ dosimeters are to be formed, break the paraffin-tetrachlorobenzene material into chunks.
- e. place about 100 g of these chunks in a beaker and remelt at about 80-100°C.
- f. screen the TLD-100 crystals through the 100 and 200 Tyler mesh screen.
- g. weigh out the proper amount of the TLD-100 crystals for use.
- h. pour a portion of the melted mixture into a 50 ml beaker and add the correct amount of TLD powder. Stir the mixture well and pour the liquid Pate into another beaker for future use.
- i. pour another 50 ml of the melted mixture into the same beaker and add the required amount of TLD powder. Pour this liquid Pate into the organ mold and allow 10-15 minutes for solidification.
- j. repeat step i, allowing for solidification, until the mold is completely filled.

At the end of the process, the complete Pate molded organ was inspected and good joining of the layers was evident. In fact, once the mixture had solidified, the individual layers were not identifiable to the naked eye. No boundaries were visible and the layered organ dosimeters exhibited similar physical characteristics to those molded at one pouring.

A distribution study similar to the one described for the first method was performed. In this experiment, the right circular cylinder of Pate was cut into 17 slices. Each slice was measured, dissolved and

the TLD crystals recovered according to established procedures. The data from this experiment are shown in Table 5. The mean concentration in the 17 slices was 1.086 ± 0.470 g of TLD powder. However, close inspection of the table indicates a problem with top four slices (slices 14-17). The high concentration in slice 14 was thought to be due to the lack of adherence to the established procedure. That is, the Pate layer was not allowed to solidify completely before subsequent layers were poured. The mean concentration in slices 1-13 was found to be 1.120 ± 0.216 g of TLD powder.

The variation of $\pm 20\%$ in the TLD distribution was an improvement over that of the previous methods. This technique was very promising and with further refinements a $\pm 11\%$ variation was achieved. However, when molding large organs, such as the liver, the horizontal distribution of the TLD crystals suffered and variations of up to $\pm 500\%$ were recorded. For this reason, the layer method was found unsatisfactory, and other procedures had to be developed to ensure a uniform distribution of the TLD powder in the organ dosimeter. This led to the molding technique described in a previous section (see Fabrication of Dosimetric Organs). Two distribution studies were conducted: in the first study, the TLD powder was added in one pouring to the Pate mixture, while in the second, the TLD powder was sprinkled while mixing. After molding and solidification, the samples were cut in chunks in different directions. Each pre-weighed chunk was placed in a beaker and the TLD powder recovered and weighed. The data from the first study are given in Table 6, while the data from the second study are given in Table 7. In the latter study, a standard deviation of 3.4% was achieved while, for the method when the TLD powder is added in one pouring, the error

Table 5. TLD Distribution Using the Layer Method for Molding

<u>Slice Number</u>	<u>Height (cm)</u>	<u>Cumulative Height (cm)</u>	<u>Total Weight (g)</u>	<u>TLD-100 Weight (g)</u>	<u>TLD Concentration (g)</u>
1	0.68	0.68	14.95150	0.19273	1.289
2	0.88	1.56	19.37895	0.24385	1.258
3	1.42	2.98	31.28255	0.43510	1.390
4	1.22	4.20	26.83448	0.35420	1.320
5	1.72	5.92	38.01695	0.34540	0.909
6	1.23	7.15	27.21747	0.21915	0.805
7	1.03	8.18	22.68863	0.24100	1.062
8	1.42	9.60	31.38180	0.38513	1.227
9	1.78	11.38	39.23075	0.43495	1.109
10	1.25	12.63	27.58180	0.20190	0.732
11	1.12	13.75	24.61440	0.24365	0.990
12	1.31	15.06	28.8653	0.40120	1.390
13	1.10	16.16	24.25600	0.26130	1.077
14	1.77	17.93	38.95190	0.93115	2.391
15	1.37	19.30	30.30130	0.27295	0.901
16	1.39	20.69	30.6400	0.11150	0.364
17	2.98	23.67	65.84770	0.16225	0.246

Table 6. TLD Distribution Using Hand-Mixing and Adding the TLD Powder to Mixture in one Batch

<u>Sample Number</u>	<u>Weight (g)</u>	<u>TLD-100 Weight (g)</u>	<u>Concentration (%)</u>
1	36.1	0.28115	0.7788
2	27.1	0.1695	0.6255
3	40.4	0.2880	0.7129
4	34.8	0.2270	0.6583
5	28.4	0.20345	0.7164
6	44.3	0.3095	0.6986
7	44.5	0.3351	0.7530
8	30.6	0.1550	0.5082
9	43.5	0.27685	0.6364
10	<u>38.5</u>	<u>0.2349</u>	<u>0.6101</u>
Total	368.2g	2.48045	Average Concentration 0.6737%

Table 7. TLD Distribution Using the Hand-Mixing Method and Adding TLD Powder by Sprinkling

<u>Sample Number</u>	<u>Weight (g)</u>	<u>TLD-100 Weight (g)</u>	<u>Concentration (%)</u>
1	81.6	0.19485	0.2388
2	51.35	0.1251	0.2437
3	60.7	0.15795	0.2602
4	51.1	0.12715	0.2488
5	43.32	0.10180	0.2350
6	64.3	0.1547	0.2406
7	72.85	0.18750	0.2574
8	88.9	0.22965	0.2583
9	54.45	0.1320	0.2424
10	<u>55.4</u>	<u>0.1390</u>	0.2509
Total	623.97	1.5497	

Average concentration in the mold } 0.2484%

Table 8. Dependence of TLD Response on TLD Concentration

<u>Sample Number</u>	<u>TLD Concentration %</u>	<u>TLD Output rel. units</u>
1	0.059	63.06
2	0.220	76.43
3	0.332	69.01
4	0.337	75.11
5	0.413	68.55
6	0.743	77.18
7	0.928	75.09
8	1.052	79.16
9	1.229	74.89
10	1.430	73.57

Mean: 73.21 ± 4.88

was \pm 11.84%. These findings explain the choice of the present dosimetric organ fabrication technique.

Dependence of TLD Response on Concentration

Because the TLD concentration in Pate varies from 0.1% to 0.5% depending on the size of the organ, a study was initiated to determine the effect of concentration on the TLD response. Eleven Pate dosimeters were fabricated, using beakers as the molds, for use in this study. Each beaker was filled with 130 g of Pate and TLD powder. The TLD concentration ranged from 0.06% to 1.43%. Sample number eleven, with a TLD concentration of 1.04%, was used as a control. The other samples were irradiated individually to the same exposure with gamma-rays, and the TLD powder recovered and read. Table 8 presents the data collected in this experiment. The mean TLD output (expressed in arbitrary units) was 73.21 with a standard deviation of 4.88. This result was within the expected range of error. However, it is thought that one source of error is the positioning error associated with this experiment. Nevertheless, these data show that there is no noticeable effect on the TLD response when the TLD concentration varies from 0.06% to 1.43%.

Effect of Pate Mixture on TLD Response:

The mixing of the TLD-100 powder with organic materials may change the thermoluminescent characteristics of the phosphor. Information on this possible effect in the literature is negligible, if not absent. Therefore, it was necessary to investigate the effects the Pate compound may have on the TLD crystals. Several studies of the TLD characteristics were conducted, and the results are reported below:

- Effect on the Glow Curve:

Pure TLD-100 powder contained in nylon capsules and TLD-100 powder in Pate were irradiated, and their glow curves were

Table 9. Effect of Usage on TLD Response

<u>Number of Cycles</u>	<u>Response of TLD in Pate (Arb. units)</u>	<u>Response of TLD in Capsules (Arb. units)</u>
0		28.01
1	24.48	32.35
2	25.47	31.26
3	25.62	34.54
4	25.37	31.25
5	27.05	32.06
6	23.91	30.83
8	23.72	30.02
12	21.74	30.35
16	21.26	27.24
22	24.58	28.77
Mean	24.32	30.61
Standard Deviation	± 1.77	± 2.08
Percent Error	7.2%	6.8%

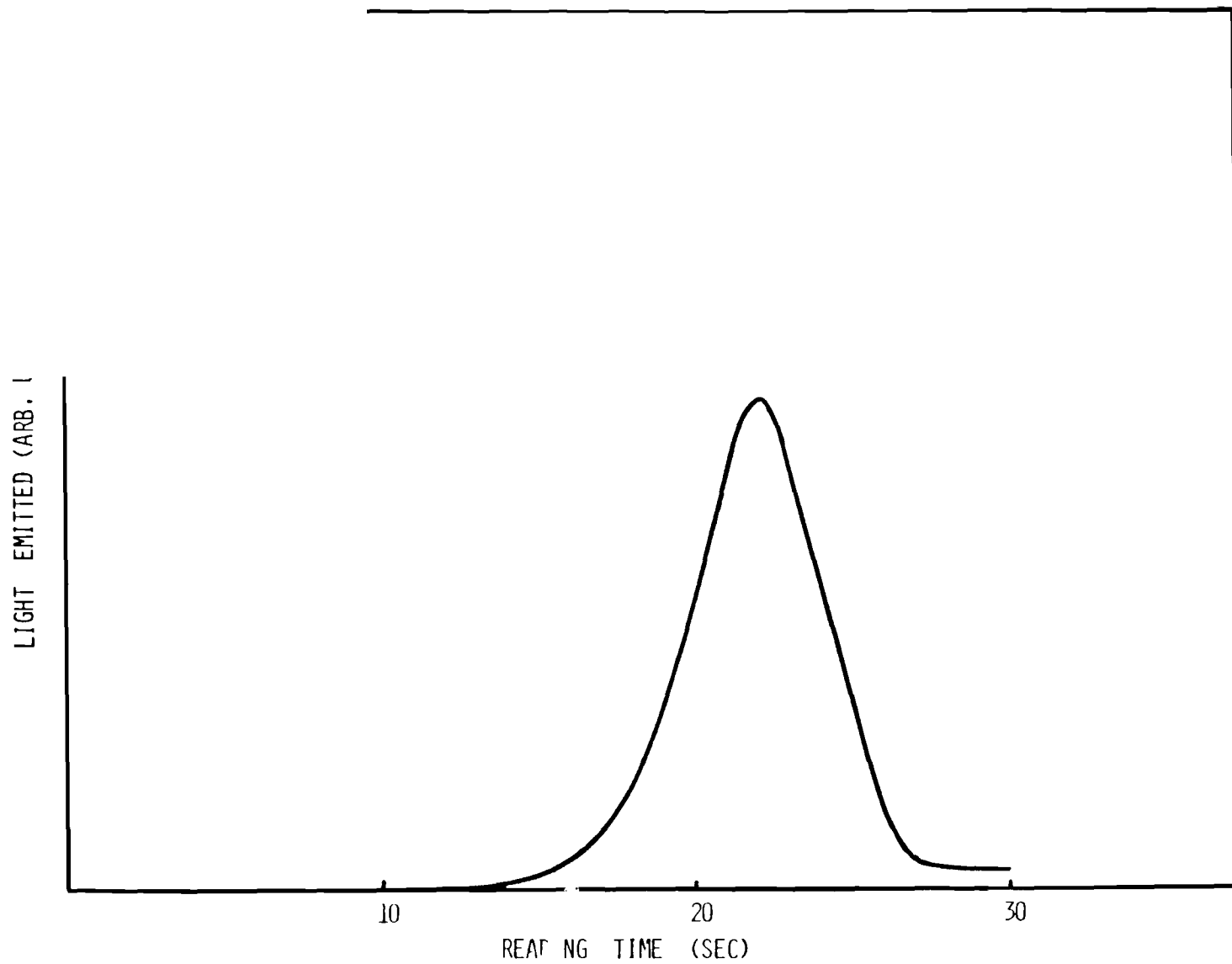


Fig. 1. Glow curve for LiF TLD-100 crystals recovered from the Pate dosimeter.

obtained (Figure 1.). Comparison of the two sets of glow curves showed no noticeable variation or effect.

- Effect of Usage on TLD Response:

In this experiment, the dependence of the TLD response on the number of uses, or the number of cycles it goes through, was studied. A sample of the TLD-100 powder was divided in two equal parts. One part was used in the Pate mixture, the other part was loaded into nylon capsules. Any apparent effect of the number of uses on the TLD response could be easily recorded by comparing the data obtained from the two different samples.

One cycle for the TLD-100 powder in capsules was defined as pre-annealing, irradiation, post-annealing, and reading. A cycle for the TLD-100 powder in Pate was defined as pre-annealing, mixing with Pate, irradiation, recovery, post-annealing, and reading. Both samples were used for 22 cycles, starting with cycle 0 for the TLD in capsules and cycle 1 for the Pate dosimeter. Cycle 0 was run to ensure an exposure which gave reasonable light output for subsequent readings. Table 9 summarizes the data obtained in this study. Although the relative light output in Pate is less than that obtained for irradiations in nylon capsules, the data indicated no effect for up to 22 cycles of use. This means, standard deviations, and the calculated percent errors were found to be within the expected range.

Effect of Contact Time on TLD Response

Two experiments were carried out to investigate the dependence of TLD response on the time of suspension in the Pate mixture. These two experiments were generally similar, except that in the

first, possible changes in the fading properties of the TLD powder were studied, while in the second, the study centered on possible effects before irradiation.

- Fading

Several sample Pate dosimeters were fabricated for this study; half of them were used as controls and the other half were irradiated individually one after the other. The TLD powder was recovered from the dosimeters and data were taken over a period of three weeks. The resulting TL fading was no more than 3% which was in agreement with the value quoted in the Harshaw data sheet.

Before Irradiation

In this investigation, two attempts were made to record any change in the TLD response due to contact with the Pate mixture before irradiation. In the first study TLD-100 was in contact with the Pate mixture for 13 days. In the second, this contact time was extended to 22 days. No noticeable effect on the TLD response was observed. The standard variation of the data was within the expected statistical error.

Response of TLD-100 Suspended in Grated Pate (Lungs)

The object of this study was to compare the response of the TLD crystals suspended in grated pate with that of the TLD crystals mixed with Pate and then the resulting compound shredded. All samples from both molding techniques were irradiated in the same manner, and there was no apparent difference in the resulting data. However, losses of TLD powder were much higher when the Pate and TLD powder were mixed, solidified, and shredded. This loss was thought to be due to pulverization of the crystals by the food processor.

Calibration Curve

A calibration curve (Figure 2), was obtained for absorbed doses between 10 mrads and 6500 rads. All exposures were carried out in a water tank in which the absorbed dose as a function of position was known accurately. Fifteen samples were read for each absorbed dose. The data, given in Table 10, for this calibration had an average standard deviation of 1.4%. The relation of TL output to absorbed dose was found to be linear up to almost 1000 rads where signs of supralinearity began to appear. Also, because of large uncertainties at low doses, it was considered that the lower limit of usefulness of the dosimeter was 20 mrads.

Energy Response:

The energy response of TLD-100 exposed in air is a known characteristic. The purpose of this investigation is to obtain a TLD energy response when the irradiation was carried out in water. Irradiation in water simulates the conditions expected when the dosimeter was used inside the phantom. This experiment was very delicate due to problems encountered in determining precisely the photon energy at different depths in a water tank. Pate samples were made small to reduce fluctuations dose to changes in photon energy as a function of depth in the phantom. Figure 3 shows a curve of the energy response of the Pate dosimeter in water. This response is very similar to that of TLD-100 in air except for the fact that there seems to be a small overresponse at low photon energies.

Table 10. Calibration Curve Data

Absorbed Dose (rads)	TL Output* (Arb. units)	Standard Deviation* (Arb. units)
$1.05 \cdot 10^{-2}$	$2.34 \cdot 10^{-1}$	0.017
$2.06 \cdot 10^{-2}$	$3.86 \cdot 10^{-1}$	0.018
$4.04 \cdot 10^{-2}$	$7.39 \cdot 10^{-1}$	0.007
$7.07 \cdot 10^{-2}$	1.182	0.011
$1.11 \cdot 10^{-1}$	1.955	0.003
$2.99 \cdot 10^{-1}$	4.955	0.054
$5.95 \cdot 10^{-1}$	10.03	0.176
$9.73 \cdot 10^{-1}$	15.95	0.05
1.94	31.71	0.36
4.86	77.75	0.94
6.74	$1.068 \cdot 10^2$	0.72
9.72	$1.551 \cdot 10^2$	0.58
19.47	$3.048 \cdot 10^2$	1.24
48.48	$7.789 \cdot 10^2$	2.33
97.05	$1.55 \cdot 10^3$	$0.04 \cdot 10^3$
$4.683 \cdot 10^2$	$7.99 \cdot 10^3$	$0.08 \cdot 10^3$
$6.556 \cdot 10^2$	$1.209 \cdot 10^4$	$0.11 \cdot 10^3$
$9.365 \cdot 10^2$	$1.764 \cdot 10^4$	$0.075 \cdot 10^3$
$2.81 \cdot 10^3$	$7.254 \cdot 10^4$	$2.42 \cdot 10^3$
$6.556 \cdot 10^3$	$2.334 \cdot 10^5$	$5.46 \cdot 10^3$

* Obtained from 15 samples at each absorbed dose.

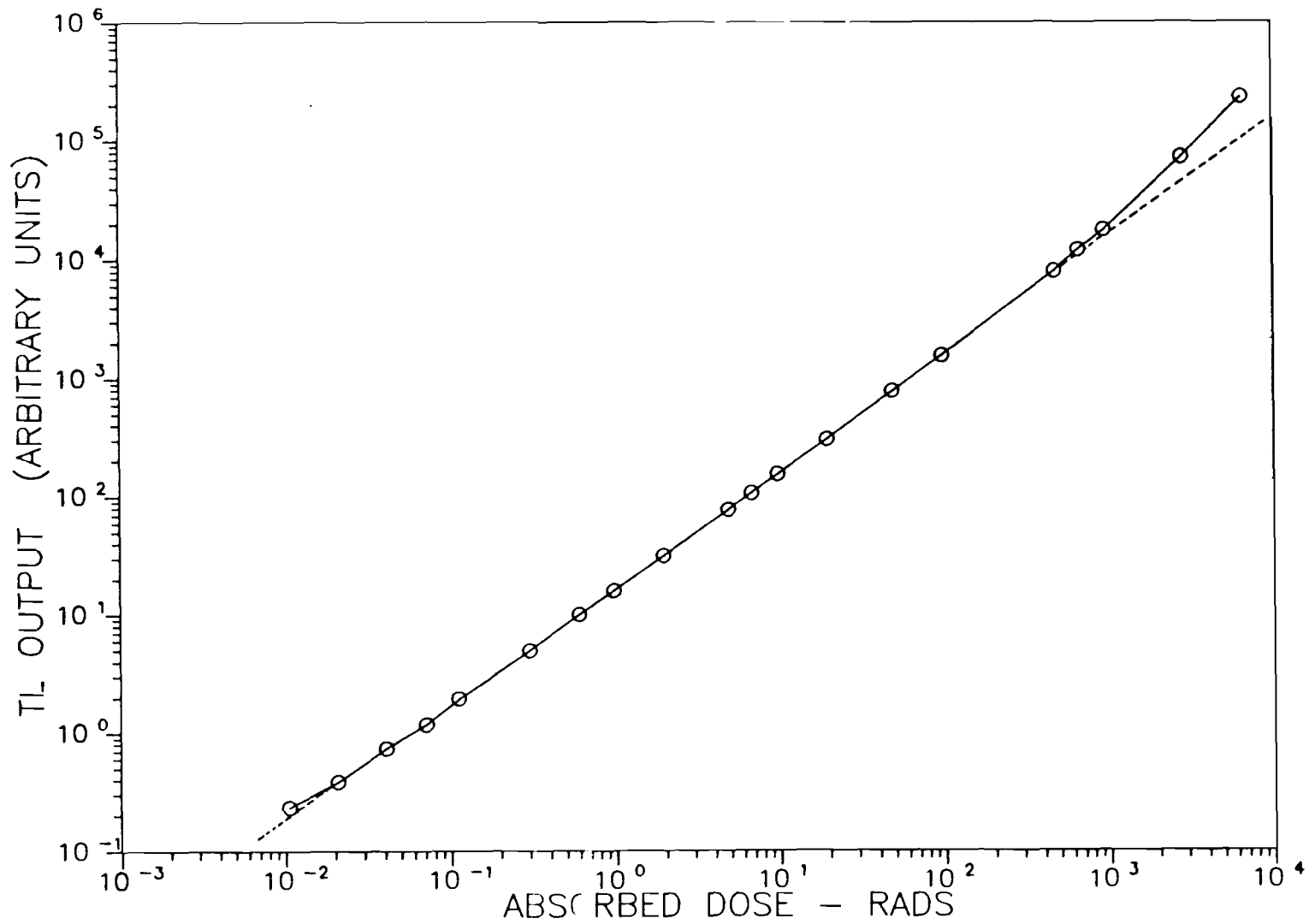


Fig. 2. Calibration curve for LiF TLD-100 crystals used in the Pate dosimeter. Calibration performed with Co-60 gamma-rays and exposures made inside a water-filled phantom.

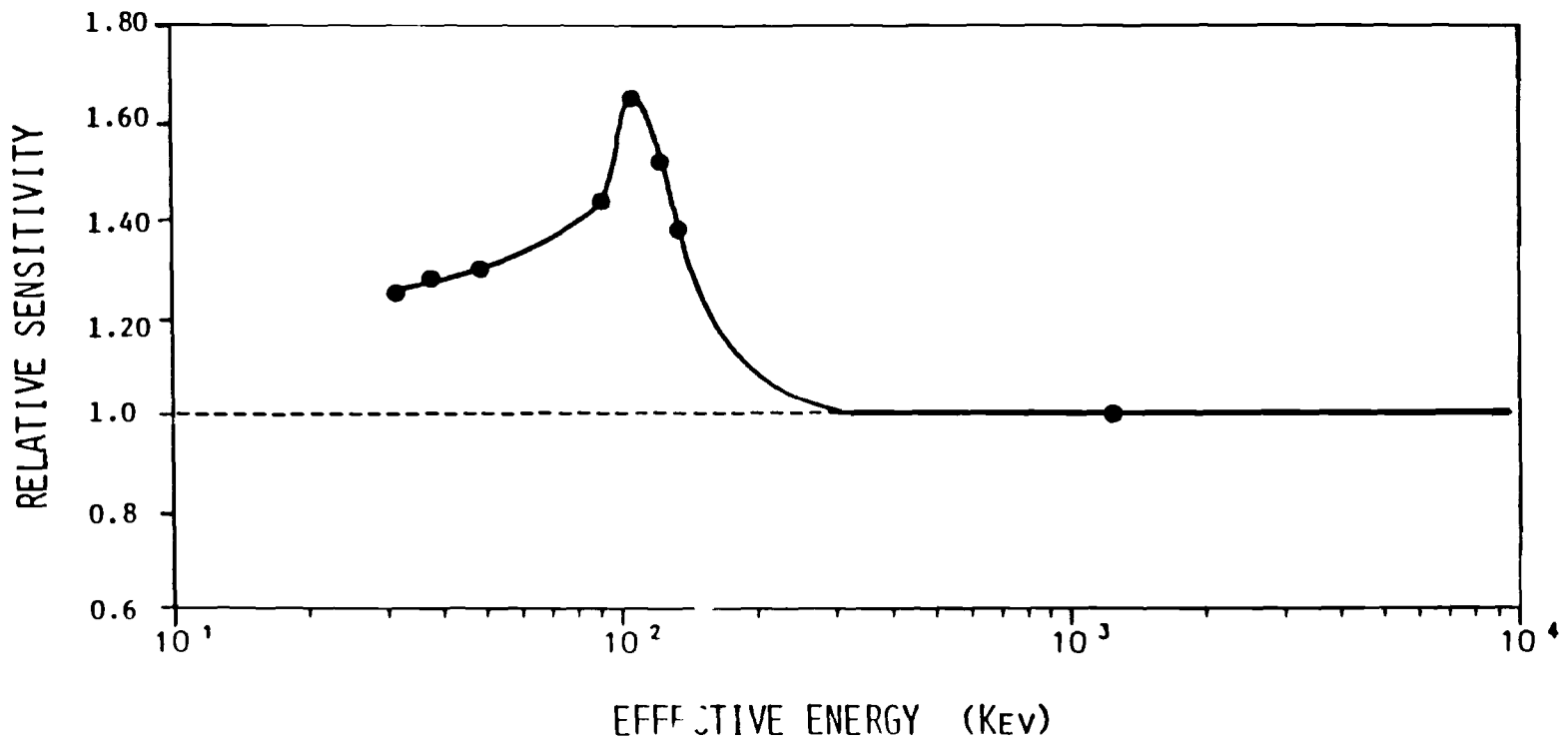


Fig. 3. Energy response of the LiF TLD-100 crystals used in the Pate dosimeter. All exposures made inside a water-filled phantom.

Errors Associated with the Dosimetric System

There are three sources of systematic error: non-uniform distribution of the TLD crystals in the organic mixture, the TLD reader-powder dispenser error, and the error associated with the TLD reading system.

The variation in the TLD concentration has been estimated to be no more than 3.5% in any part of any organ. Even though this variation does not translate automatically to a 3.5% standard deviation in the measurement of the absorbed dose, it was assumed that it represents at the most an average value.

The error associated with the powder dispenser has been estimated to be of the order of 2.9%, which is higher than expected from an electrically vibrated dispenser. This large error was thought to be due to the fact that thousands of samples had to be read, and consequently, errors associated with the powder dispenser had a strong influence on the final error associated with the experiment.

The last source of error was due to the reading system itself, including the positioning of the pan containing the TLD powder on the tray. Throughout this study, an average standard deviation of 3% was achieved for doses ranging from 20 mrad to 1000 rads.

Therefore, and in summary, the total error associated with the dosimetric system can be estimated to be about 9.4%. This result and the characteristics described in previous sections make the Pate dosimeter a suitable choice to perform the necessary internal dose measurements.

B. Preparation of Molds

To prepare the Pate dosimeter described in A. above it was necessary that molds be fabricated which resembled the organs of interest as closely as possible. Several techniques were studied and much of this work has been described in previous reports.

Organs for use in this study were fabricated in the following manner. A computer routine (22) was used to plot-out cross-sections of the mathematical phantom at 1 cm intervals along the vertical axis of the phantom. Organs, for which organ molds were required, were identified and cut out of the printout paper. These organ shapes were traced on hardwood boards (1 cm thick). The shapes were cut out, assembled, and fabricated to create positive replicas of the mathematical organs (see Fig. 4).

The dosimetry technique suggested by Feher et al. (13) requires a negative mold to produce a dosimeter which matches the organ shape. Even though the PAC dosimeter these authors described was discarded in favor of the Pate dosimeter, a negative mold was still required for each organ. A negative mold (or container) was also needed for organs which would contain the radioactive source material. Fabrication of these source organ containers will be discussed also in this section.

Plaster Bandage Molding

Several molding techniques were considered including plaster of paris - stone casting, vacuum plastic molding, and plaster bandage molding. The latter technique was selected because it was inexpensive, was relatively rapid, and the mold properties were superior to those obtained by other methods.

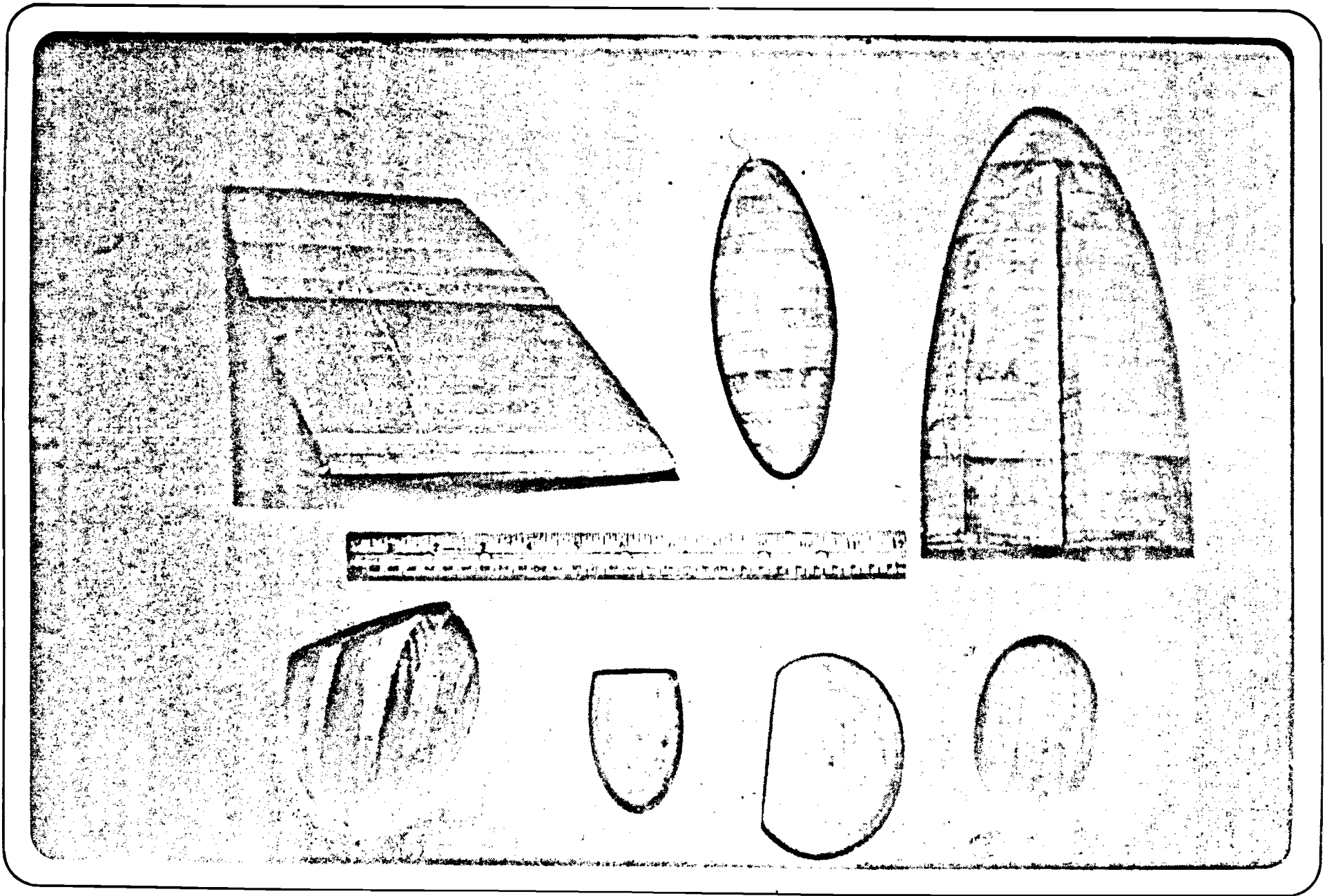


Fig. 4. Wooden models of the mathematical organs.

The procedure for forming negative organ molds is as follows. A hardwood mold was pre-treated with a thin film of silicon lubricant to provide easy removal of the plaster mold. Several layers of quick-settling plaster bandages* were mixed with water and wrapped around the pre-treated mold. Bandages were applied to the mold until a layer approximately 2 cm thick was formed. The plaster "cast" was allowed to harden for a short time, at room temperature, until it was sufficiently rigid to be cut. Then the cast was cut into two pieces for future removal of the organ mold. However, the mold was allowed to set-up completely for more than 18 hr., at room temperature, with the positive mold still inside to avoid shrinkage and assure structural integrity.

After removal of the positive organ mold the two halves of the plaster (negative) mold were rejoined and held together with additional strips of plaster bandage (see Figure 5). These negative molds, produced by the above procedures, were used to form the required volumetric dosimeters (see Figure 6).

Section A of this report indicates a deviation from this procedure when forming the volumetric dosimeter. This change was dictated by the non-uniform distribution of TLD powder when the Pate-TLD mixture was poured into the plaster organ mold. However, the new molding procedure still uses plaster bandage molds produced as described above.

Fiberglass Molding

Organ replicas also were required to contain radioactive materials when the organ was assumed to be a "source organ". In this

*Johnson and Johnson Products, Inc., New Brunswick, New York 08903.

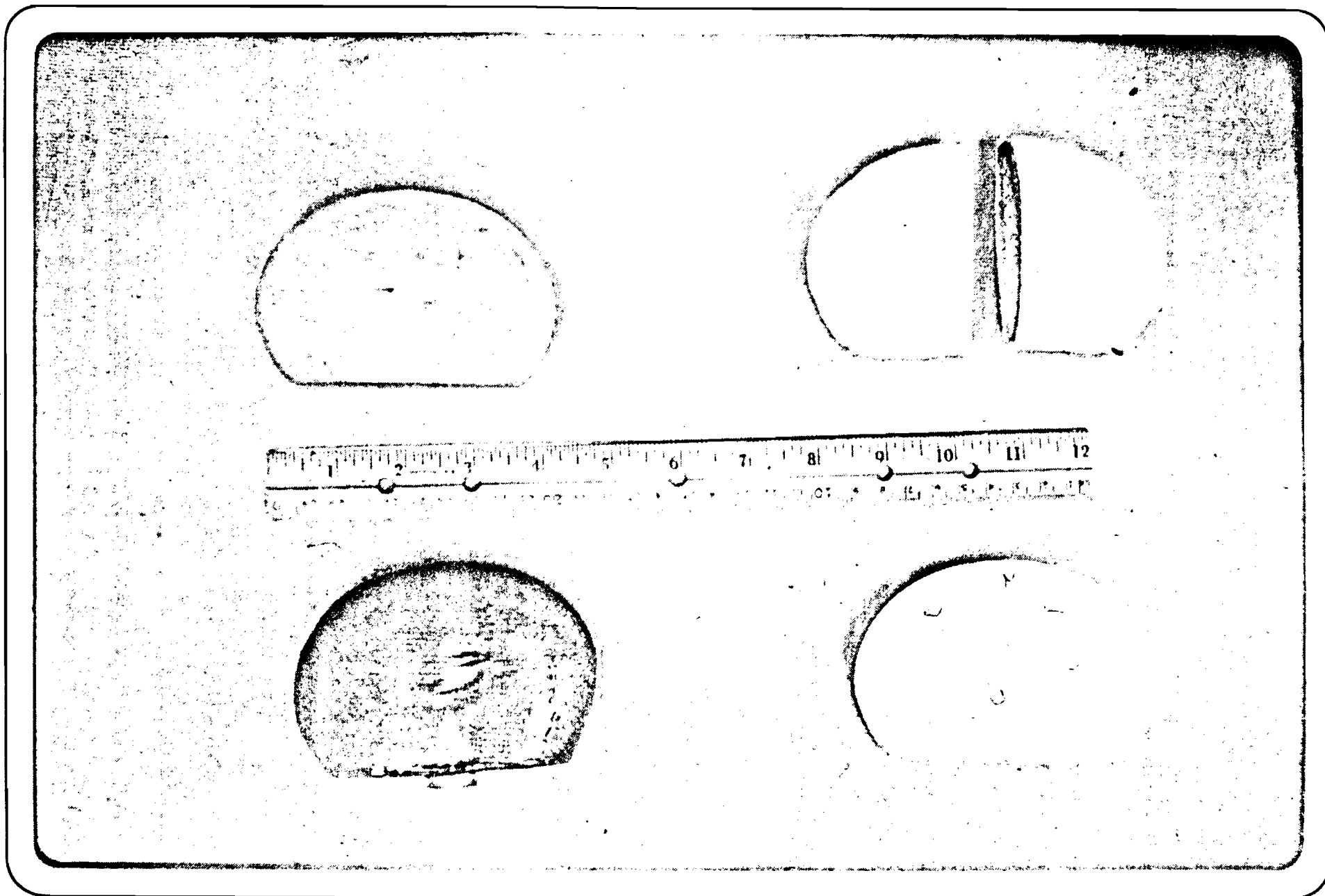


Fig. 5. Kidney molds. Top: wooden mold and plaster bandage mold,
Bottom: fiberglass mold and volumetric dosimeter.

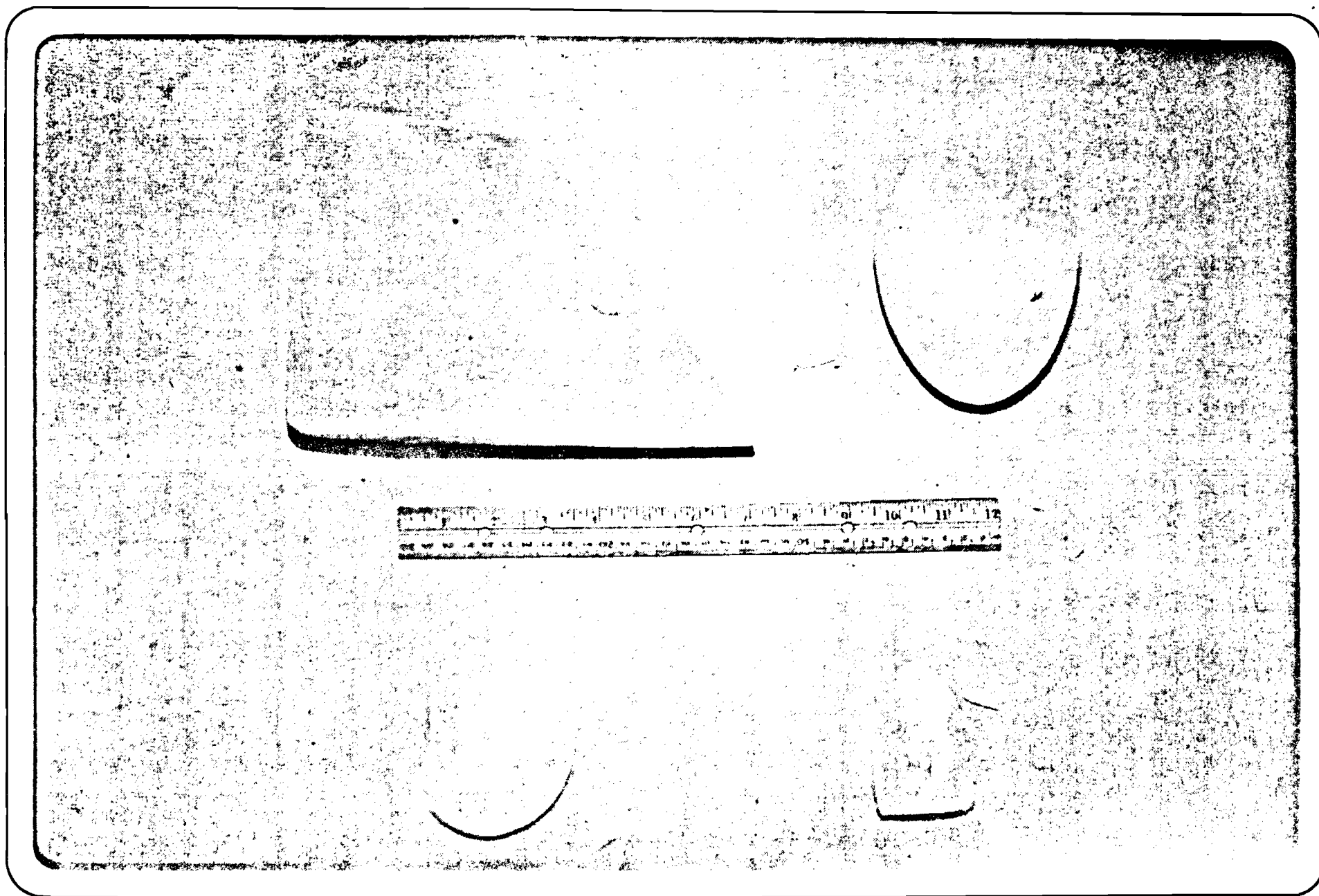


Fig. 6. Volumetric dosimeters. (top: liver and heart, bottom: kidney and uterus)

case, plaster bandage molding was not appropriate. A strong, thin, lightweight source organ replica was required for this purpose. In addition, it was necessary to be able to seal the source organs to prevent leakage of the contained radioactive material into the liquid-filled phantom (during use) or into the shielded well (during storage).

Fiberglass was selected as a material which met the above criteria. In addition, strips of fiberglass could be laid down over the wooden positive organ molds in a fashion similar to the plaster-bandage molding technique. The resulting fiberglass replica was strong, lightweight and was faithful to the organ mold around which it was formed.

Fiberglass organ replicas were formed for the kidneys, lungs, liver, bladder, uterus, and stomach. These replicas were fitted with lucite openings and screw-plugs to allow easy filling and sealing. In most cases, other lucite attachments had to be added to the outside of the source organ replicas to allow positive positioning inside the trunk of the phantom, and to ensure their structural integrity (see Figure 7).

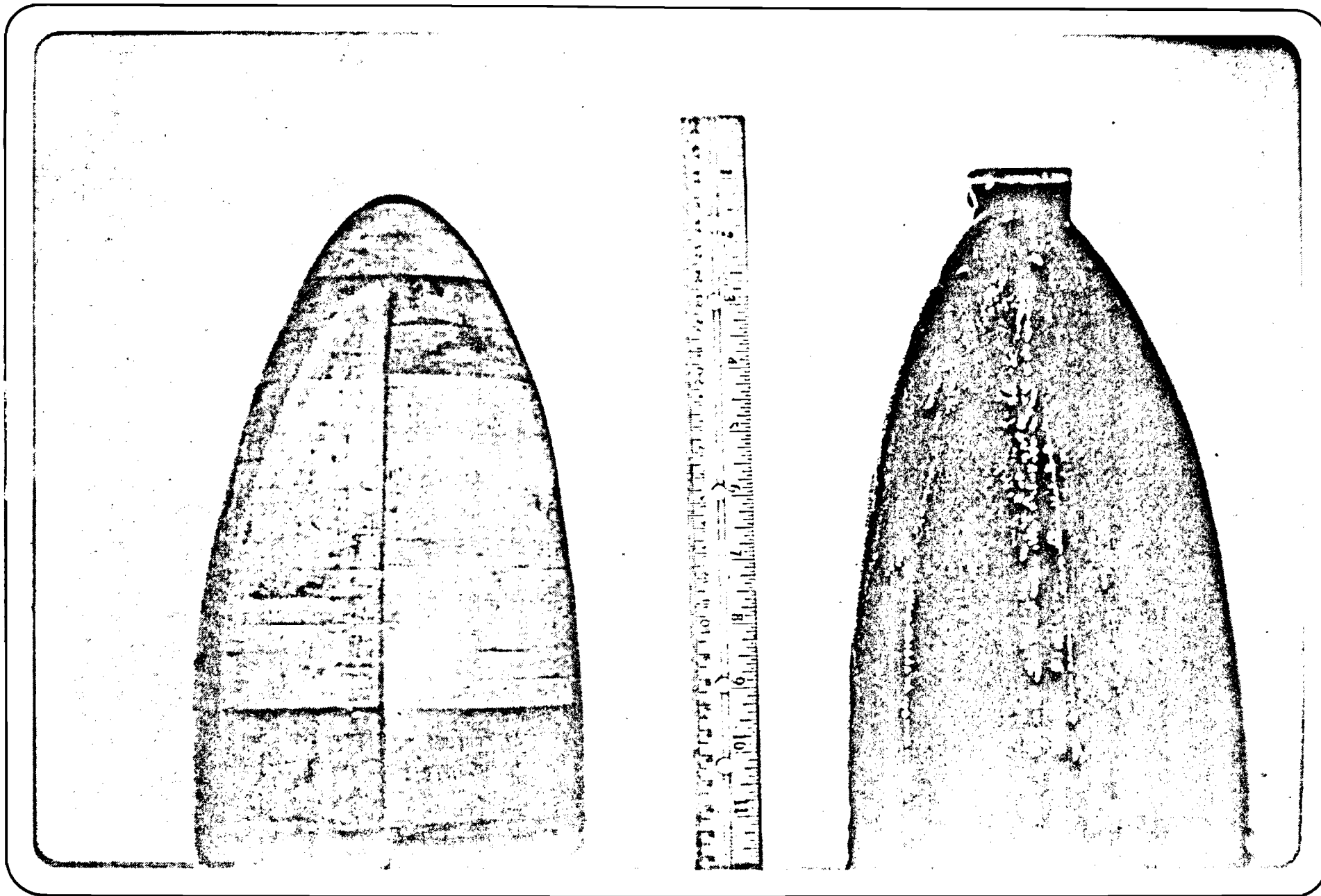


Fig. 7. Wooden and fiberglass molds of the right lung.

C. Source Organ Fabrication

Organs containing radioactive material (i.e., source organs) were fabricated for use in this experiment. The radionuclide Co-60 was selected for use in the initial experiments for several reasons. First, the radionuclide had a long half-life and decay corrections over the 1-2 day exposure period in each experiment were not required. Second, high energy photons emitted in the decay allowed measurements of absorbed dose to organs at relatively large distances from the source organ. Third, use of Co-60 provided a link between these experiments and those of Garry, et al. (5) and Mei et al. (6).

The Co-60 to be used in these experiments was produced by neutron activation in the Georgia Tech Research Reactor (GTRR). The substance to be irradiated was cobaltous nitrate ($\text{Co}(\text{NO}_3)_2 \cdot 6 \text{H}_2\text{O}$) which contained 20.25% of the isotope Co-59. This isotope is 100% naturally abundant so the production of other isotopes of cobalt was not of concern in the irradiation. Other activation products (e.g., nitrogen or oxygen) which might be produced during the irradiation had short half-lives and were not expected to pose any problem. In addition, cobaltous nitrate was selected because the compound was readily soluble in water.

An activity of 10 mCi was selected as appropriate for each source organ. This activity was selected because irradiations could be accomplished in a reasonable period. At the same time it was felt that this level of activity could be handled safely and with a minimum of exposure to personnel fabricating the source organs. To produce these levels of activity the GTRR has to be operated for periods varying between 4 and 8 hours depending on the size of the organ. After irradiation the Co-60 was stored for 2-4 weeks before source organs were fabricated. This storage period

allowed for the decay of any short lived radionuclides which may have been produced during the irradiation.

In general, fabrication of all source organs followed the same procedures. Total volumes of solutions, etc. were a function of the source organ volume. All steps of the procedure were carried out in a chemical hood which contained a shielded sink. In addition, certain steps in the procedure used a small gloveless box placed inside the hood. Procedures for source organ fabrication are as follows:

1. Transfer rabbit from the transport cask to the beta shield in the hood.
2. Insert beta shield in left-hand part of the gloveless box (in the bottom of the shielded sink). Leave these inside the hood for a future survey.
3. Using tool, open the rabbit and dump out the inner container.
4. Remove hand bringing out the beta shield containing the rabbit (left hand) and the rabbit top and opening tool (in right hand).
5. Step back to allow a radiation survey.
6. Grip inner container with tongs and vent it by inserting the large hypodermic needle in the top.
7. Using the needle as a handle, remove the container from the gloveless box and place the container on absorbent paper in the corner of the sink.
8. Remove the glove box from the sink but do not remove from the hood.
9. Place a 500 ml beaker into the sink - upside down. Cover bottom of beaker with a small piece of absorbent paper.
10. Place a 250 ml beaker into the sink.

11. Using the tongs and the large beaker as a rest, cut open the small container.
12. Place the small container in the 250 ml beaker, remove the hypodermic needle.
13. Step back to allow a radiation survey.
14. Add to the beaker approximately 150 ml of distilled water.
15. Allow about 10-15 minutes for the material to dissolve.
16. Remove capsule from the beaker, use a small piece of absorbent paper to contain any possible liquid contamination. Discard both in hot waste.
17. Take a sample of the solution with a pipette and transfer to a beaker containing a known amount of distilled water. (The sample taken is usually either 0.5 or 1 ml depending on the size of the organ. The volume of distilled water is selected based on the desired activity.) Wash the pipette repeatedly with water from the beaker. Take 10 - 1 ml aliquots from the beaker and transfer to 10 stainless steel planchets. Dry the planchets under a heat lamp and count the samples before proceeding to fill the source organ container. If activity is found to be acceptable proceed with step 18.
18. Place stand (with funnel) in the bottom of the sink.
19. Position source organ under the funnel. Make sure the funnel tip is inserted partially (3-4mm) into the source organ opening.
20. Pour the cobalt-60 solution into the source organ.
21. Pour a gelatin solution (gelatin, water and thymol blue) into the beaker which contained the cobalt-60 solution.
22. Pour this solution into the source organ.

23. The beaker and funnel may be rinsed into the source organ if the organ is not completely full. Move funnel out of the way - be aware of liquid drops remaining on the funnel tip.
24. Seal organ by inserting the threaded plug. CAUTION - This does not seal the organ completely since the plug has a small hole in it to allow air to escape. Wipe the plug with a small piece of absorbent paper to insure the surface is dry and can be sealed.
25. Seal the plug securely with fiberglass resin and allow it to set-up.
26. Do a wipe test on the outside of the source organ.
27. Remove the source organ from the hood using a suitable container and place in storage for future transfer to the experimental area.

This procedure was used for fabrication of the bladder, stomach, liver, kidneys, and uterus source organs. The gelatin added in step 21 transformed the Co-60 solution into a semi-liquid form which was less likely to be spread widely over an area if the source organs were fractured violently.

Calibration of the source organs consisted in evaluating the 10 stainless steel planchets (obtained in step 17 of the source organ fabrication procedure) of each source organ. The detection system involved a Ge(Li) detector calibrated with a NBS mixed radionuclide standard. Table 11 gives the activity of each source organ used in this research. Also included in this table is the percent error associated with each activity, characterized by the coefficient of variation (CV).

It can be seen from Table 11 that the bladder and the stomach source organs) had a relatively high coefficient of variation (compared to the other four source organs) associated with their activities. These two source organs were the first to be fabricated, and at the time they were

Table 11. Activities of the Source Organs Used
in the Absorbed Dose Measurements.

Source Organ	Activity (mCi)	C.V. ^a (%)
Bladder	8.674	10.00
Left Kidney	11.277	7.39
Right Kidney	12.189	1.57
Liver	12.117	0.50
Stomach	8.611	10.00
Uterus	9.115	1.98

a) C.V. = $100 \times \frac{\text{Standard Deviation}}{\text{mean}}$

made, a slightly different fabrication procedure was used. This procedure included a variation in step 17 from the procedure given above. This variation consisted of taking sample from the highly radioactive solution with a pipette, and dropping approximately 0.05 ml of the sample in each stainless steel planchet. This resulted in two types of errors: the inability to measure the 0.05 ml aliquot within certain limits of accuracy, and an increase of the detector's percent dead time when reading the high activity in each planchet.

The activities of the other four source organs were calculated within acceptable limits of accuracy. Their average coefficient of variation is 2.86%, which brings the total average coefficient of variation for all six source organs to 5.24%.

D. Results

Phantom Preparation:

Because of the high source organs activities involved, special measures were taken to comply with the federal and local regulations concerning the handling of radioactive materials. For this reason, the phantom Mr. ADAM, was placed in a shielded room, and surrounded with additional shielding to reduce the radiation levels outside the room. The phantom was assembled, with the bone region in place. The head and the legs tissue regions were filled with water, while the trunk region was partially filled to allow for positioning of the various target and source organs.

In-phantom measurements were made for six different source organs, namely the stomach, bladder, liver, uterus, left kidney, and right kidney. Two absorbed dose measurements were taken for each of these source organs, except for the left kidney, which was used only once as a source organ.

The loading order of the target and source organs in the phantom varied from one source organ to another. This order was selected to limit, as much as possible, human exposure to radiation, considering that the source organs had to be handled by hand. The average time of loading and unloading a source organ was approximately 45 sec. The phantom loading procedure is given in Table 12 for each source organ used in this research; the source organ is underlined to point out its order of loading.

Once all the target and source organs were loaded, the trunk was completely filled with water. Then, the head was positioned on top of the trunk base. The time of irradiation for each measurement was set such that the TL reading of the target organ expected to receive the least amount of

Table 12. Irradiation Times for the Absorbed Dose Measurements.

Source Organ	Irradiation Time (hrs)	
	Measurement-1	Measurement-2
Bladder	22.75	24.55
Left Kidney	25.17	-
Right Kidney	19.50	14.42
Liver	23.92	19.27
Stomach	24.06	20.92
Uterus	22.38	21.24

exposure would be statistically acceptable. Table 13 gives the average time of irradiation for each source organ. The data presented in this chapter were taken over a period of two weeks.

Results of Measurements

After the irradiation is completed, the organs are removed in a reverse order as they were loaded. The source organ is taken back immediately to the storage room to avoid any unwanted irradiation of the target organs. Each target organ was cut in small chunks to speed up the recovery of the TLD powder, following the procedure described in the preceding chapter. Then, each organ's TLD powder was post-annealed for 10 minutes at 100°C, after which it was ready to be read. Before each organ's evaluation, the sensitivity of the TLD reader was checked and recorded to allow for future correction of the data. This correction was needed because, even after the TLD crystals are recovered, they still contain invisible amount of Pate. Therefore, when reading these crystals, the organic impurities evaporate and deposit on the filter of the photomultiplier tube. This deposition leads to a decrease of the sensitivity of the TLD reader over time. However, this loss of sensitivity can be estimated using the ^{14}C light source of the TLD reader, which results in the determination of a correction factor relative to the condition of the TLD reader when the calibration curve of the TLD powder was generated. This correction factor was then applied to the TL reading of each target organ.

Ten readings were taken for each target organ. With the resulting mean, the average absorbed is determined by using the calibration curve and its characteristic equation, given in chapter III. The corresponding "S" factor is calculated using the following equation:

$$S (r_2 \leftarrow r_1) = \frac{\bar{D} (r_2 \leftarrow r_1)}{A_1 t}$$

Table 13. Loading Sequence of the Organs in Mr. ADAM

Source Organ	Loading Sequence
Bladder	right kidney, left kidney, liver, right lung, <u>BLADDER</u> , uterus, left lung, and heart.
Left Kidney	uterus, right kidney, liver, right lung, <u>LEFT KIDNEY</u> , left lung, and heart.
Right Kidney	uterus, left kidney, liver, left lung, <u>RIGHT KIDNEY</u> , right lung, and heart.
Liver	uterus, right kidney, left kidney, left lung, <u>LIVER</u> , right lung, and heart.
Stomach	uterus, right kidney, liver, right lung, left kidney, <u>STOMACH</u> , left lung, and heart.
Uterus	right kidney, left kidney, liver, right lung, <u>UTERUS</u> , left lung, and heart.

where, A_1 is the source organ activity given in Table 11, in μCi , and t is the irradiation time, in hrs.

The experimental "S" factors for the various source-organ configurations are given in Table 14 through Table 19.

Theoretical Results

To calculate the absorbed fractions using the MIRD technique, the computer code ALGAM (described in chapter II) had to be adapted to simulate the experimental conditions. This adaptation was made possible by:

1. incorporating the mathematical equations which define the experimental phantom, Mr. ADAM, in place of those defining the MIRD phantom; and by
2. changing the program size of the code to accommodate the larger number of media (six) that constitute Mr. ADAM. The chemical composition of all these six media was specified in the input data file of the code.

The code was run for each source organ, using 60,000 photon histories. The resulting "S" factors were calculated as follows:

$$S(r_2 \leftarrow r_1) = \Delta_1 \phi_1 + \Delta_2 \phi_2$$

In the case of ^{60}Co source organs which were used in this research,

$$\Delta_1 = 2.503 \text{ g-rad}/\mu\text{Ci-hrs} \text{ for photon energies of } 1.173 \text{ MeV,}$$

$$\Delta_2 = 2.842 \text{ g-rad}/\mu\text{Ci-hrs} \text{ for photon energies of } 1.332 \text{ MeV.}$$

The calculated "S" factors are given in Table 14 through Table 19.

Table 14. Comparison Between Calculated and Measured S Factors for a Uniformly Distributed Cobalt-60 Source in the Bladder.

Target Organ	Mass of Organ (g)	Calculated S Factor	C. V. ^a (%)	Measured S Factor	Percent Variation ^b
Heart	552	.1843E-05	19.58	.1664E-05	+9.71
Left Kidney	125	.1412E-04	15.65	.9009E-05	+36.20
Right Kidney	125	.1151E-04	15.36	.8786E-05	+23.67
Liver	1683.6	.7513E-05	5.87	.5714E-05	+23.95
Left Lung	504.3	.1279E-05	22.72	.1836E-05	-43.55
Right Lung	504.3	.2128E-05	21.00	.1834E-05	+13.82
Uterus	73.6	.2210E-03	5.39	.1861E-03	+15.79

a C. V. is the coefficient of variation of the S Factor

b Percent Variation = $\frac{\text{Calculated S Factor} - \text{Measured S Factor}}{\text{Calculated S Factor}} \times 100$

Table 15. Comparison Between Calculated and Measured S Factors for a Uniformly Distributed Cobalt-60 Source in the Left Kidney.

Target Organ	Mass of Organ (g)	Calculated S Factor	C. V. ^a (%)	Measured S Factor	Percent Variation ^b
Heart	552	.1251E-04	7.99	.9627E-05	+23.03
Left Kidney	125	.2469E-02	1.26	-	-
Right Kidney	125	.5787E-04	8.05	.4295E-04	+25.78
Liver	1683.6	.2670E-04	3.20	.1962E-04	+26.50
Left Lung	504.3	.1474E-04	7.44	.1304E-04	+11.53
Right Lung	504.3	.7224E-05	10.63	.5259E-05	+25.82
Uterus	73.6	.2523E-04	14.21	.2209E-04	+12.45

a C. V. is the coefficient of variation of the S Factor

b Percent Variation = $\frac{\text{Calculated S Factor} - \text{Measured S Factor}}{\text{Calculated S Factor}} \times 100$

Table 16. Comparison Between Calculated and Measured S Factors for a Uniformly Distributed Cobalt-60 Source in the Right Kidney.

Target Organ	Mass of Organ (g)	Calculated S Factor	C. V. ^a (%)	Measured S Factor	Percent Variation ^b
Heart	552	.1492E-04	7.49	.1259E-04	+15.62
Left Kidney	125	.6363E-04	7.71	.4244E-04	+33.30
Right Kidney	125	.2410E-02	1.28	-	-
Liver	1683.6	.1087E-03	1.68	.8485E-04	+21.94
Left Lung	504.3	.7897E-05	10.80	.7595E-05	+3.82
Right Lung	504.3	.1828E-04	7.24	.1512E-04	+17.29
Uterus	73.6	.3703E-04	13.12	.2373E-04	+35.92

a C. V. is the coefficient of variation of the S Factor

b Percent Variation = $\frac{\text{Calculated S Factor} - \text{Measured S Factor}}{\text{Calculated S Factor}} \times 100$

Table 17. Comparison Between Calculated and Measured S Factors for a Uniformly Distributed Cobalt-60 Source in the Liver.

Target Organ	Mass of Organ (g)	Calculated S Factor	C. V. ^a (%)	Measured S Factor	Percent Variation ^b
Heart	552	.2516E-04	5.74	.2842E-04	-12.96
Left Kidney	125	.2689E-04	11.91	.2058E-04	+23.47
Right Kidney	125	.9317E-04	6.38	.9026E-04	+3.12
Liver	1683.6	.4221E-03	8.02	-	-
Left Lung	504.3	.1145E-04	8.51	.1344E-04	-17.38
Right Lung	504.3	.4086E-04	4.82	.4191E-04	-2.57
Uterus	73.6	.1604E-04	18.56	.1378E-04	+25.75

a C. V. is the coefficient of variation of the S Factor

b Percent Variation = $\frac{\text{Calculated S Factor} - \text{Measured S Factor}}{\text{Calculated S Factor}} \times 100$

Table 18. Comparison Between Calculated and Measured S Factors for a Uniformly Distributed Cobalt-60 Source in the Stomach.

Target Organ	Mass of Organ (g)	Calculated S Factor	C. V. ^a (%)	Measured S Factor	Percent Variation ^b
Heart	552	.2609E-04	5.68	.1685E-04	+35.42
Left Kidney	125	.8206E-04	6.69	.5989E-04	+27.02
Right Kidney	125	.2649E-04	10.44	.1903E-04	+28.16
Liver	1683.6	.3661E-04	2.80	.2516E-04	+31.28
Left Lung	504.3	.3088E-04	5.44	.2504E-04	+18.91
Right Lung	504.3	.1109E-04	8.50	.8540E-05	+22.99
Uterus	73.6	.2072E-04	14.44	.1554E-04	+25.00

a C. V. is the coefficient of variation of the S Factor

b Percent Variation = $\frac{\text{Calculated S Factor} - \text{Measured S Factor}}{\text{Calculated S Factor}} \times 100$

Table 19 . Comparison Between Calculated and Measured S Factors for a Uniformly Distributed Cobalt-60 Source in the Uterus.

Target Organ	Mass of Organ (g)	Calculated S Factor	C. V. ^a (%)	Measured S Factor	Percent Variation ^b
Heart	552	.3495E-05	15.23	.3043E-05	+12.93
Left Kidney	125	.2559E-04	11.39	.2316E-04	+9.50
Right Kidney	125	.3000E-04	10.68	.2358E-04	+21.40
Liver	1683.6	.1771E-04	3.92	.1228E-04	+30.66
Left Lung	504.3	.3119E-05	15.98	.3263E-05	-4.62
Right Lung	504.3	.2963E-05	15.86	.2735E-05	+7.69
Uterus	73.6	.3833E-02	1.33	-	-

a C. V. is the coefficient of variation of the S Factor

b Percent Variation = $\frac{\text{Calculated S Factor} - \text{Measured S Factor}}{\text{Calculated S Factor}} \times 100$

E. Discussion of Results

Error Estimate:

There are seven possible sources of errors which are related to the measurements of absorbed doses. These errors arise from:

1. the Pate dosimeter;
2. the TLD reading system;
3. the molding technique used to fabricate the dosimetric organs;
4. the activity in each source organ;
5. the positioning of the different source and target organs;
6. the irradiation time; and
7. the statistical evaluation inherent in the dose measurements themselves.

The first two sources of errors were discussed in great detail in section A. The combined error from both the Pate dosimeter and the TLD reading system was estimated to be at the most 9.4%.

The error associated with the molding technique can be evaluated by comparing the dimensions of the wooden organs (the equations describing these wooden replicas are given in Appendix I) with those of the dosimetric and source organs. Several investigations were made to study the reproducibility of the plaster bandage mold, and its effect on the shape and size of the molded organs. The results indicated that if the plaster bandage mold is rigid enough (made of several layers of plaster bandage), the variation of the dimensions of the molded organs is no more than 1%.

The activity of each source organ was given in Table 11, including the error associated with each activity. The value of this error varies from one source organ to another. However, to simplify the estimate of a total

error for the absorbed dose measurements, an average uncertainty of the activity in all source organs was computed and evaluated to be of the order of 5.24%.

The error related to the positioning of the different source and target organs was reduced to a negligible value by using fixed supports to hold the organs in Mr. ADAM. These supports remained in the phantom during the entire period the absorbed dose measurements were made. The placement of the various organs using the supports altered the initial mathematical equations describing the positioning of these organs, however, all changes were included in the final equations given in Appendix I.

The error associated with the irradiation time is also almost nil. This is due to the fact that most irradiation times for the measurements were of the order of 20 hours, while the period of loading and unloading a particular source organ is no more than 90 seconds. Therefore, any uncertainty on the irradiation time is assumed negligible.

Finally, the statistical error inherent in the absorbed dose measurements themselves can be evaluated in terms of the distribution of the data for each in-phantom irradiation. A standard deviation was calculated for each target organ-source organ configuration. Two measurements were made for each source organ, except for the left kidney, and the average coefficient of variation for all target organs was approximately 2.5%. In the case of the left kidney source organ experiment, the average coefficient of variation was of the order of 4%. To conclude this paragraph on the statistical error, it should be noted that the corresponding coefficient of variation depends on all the other six sources of errors discussed previously.

Therefore, the average percent error for the absorbed dose measurements can be computed in two steps: first, by adding the coefficients of variation of all independent errors, and second by applying the square root of the sum of squares method to include the dependent errors. Using this rule, the average percent error is at the most 16%.

Comparison of Calculated and Measured Absorbed Doses

Comparison of calculated and measured "S" factors for 6 target organs-7 target organs configurations were given in Table 14 through Table 19. Without considering the experimental error, it can be seen from these tables that:

1. All coefficients of variation (CV) are less than 25%. (the level of rejection of the Monte Carlo data set by the MIRD Committee), and therefore, all calculated "S" factors are statistically acceptable; and
2. the calculated "S" factors are generally higher than the measured "S" factors, as indicated by the percent variation data.

However, this last statement becomes invalid when one takes into account the experimental uncertainty. This is shown in Table 20 which gives the average percent variation between calculated and measured "S" factors, and the percent error of the measurements for each source organ experiment. The average coefficient of variation and the average percent variation were determined for each source organ by computing the mean of the coefficients of variation (C.V.) and the percent variations for the corresponding target organs, respectively (see Table 13 through Table 19). The calculation of the percent error of the measurements was based on the error analysis discussion presented in the preceding section.

Table 20. Error Estimates and Percent Variation of the "S" Factors Data for Each Source Organ Study.

Source Organ	Calculated C.V. (%)	"S" Factors ^a % Variation	Experimental % Error
Bladder	15.08	+ 11.37	20.55
Left Kidney	8.59	+ 20.85	18.23
Right Kidney	8.01	+ 21.32	12.23
Liver	9.32	+ 3.24	11.18
Stomach	7.70	+ 26.97	20.55
Uterus	12.80	+ 12.92	12.63

a) See data tables for the definition of the % Variation

From Table 20, the data indicate the existence of an agreement between calculated and measured absorbed doses for all 6 source organ studies. However, this agreement is in "one direction" because there is a slight indication that the Monte Carlo calculations may overestimate internal absorbed doses by few percentage points. This result applies also to two previous attempts to verify the MIRD internal dose calculations. In fact, after reanalysis of the data reported by Garry et al. (Ga74) and Mei et al. (Me75), it was found that in the majority of the source organ-target organ configurations, the calculated absorbed fractions were a little higher than the measured absorbed fractions. Therefore, it can be said that the MIRD method may be a little "conservative" in calculating internal absorbed doses. If this is the case, we know at least that by using the Monte Carlo data correctly, human life was not endangered by under-estimating the absorbed doses.